

LiDAR Remote Sensing Meets Weak Supervision: Concepts, Methods, and Perspectives

Yuan Gao^{a,b,c,1}, Shaobo Xia^{d,1}, Pu Wang^e, Xiaohuan Xi^{a,b,c}, Sheng Nie^{a,b,c,**}, Cheng Wang^{a,b,c,**}

^aKey Laboratory of Digital Earth Science, Aerospace Information Research Institute, Chinese Academy of Sciences, Beijing 100094, China

^bInternational Research Center of Big Data for Sustainable Development Goals, Beijing 100094, China

^cUniversity of Chinese Academy of Sciences, Beijing 100094, China

^dThe Department of Geomatics Engineering, Changsha University of Science and Technology, Hunan 410004, China

^eInstitute of Energy, Environment, and Economy, Tsinghua University, Beijing 100084, China

Abstract

LiDAR (Light Detection and Ranging) enables rapid and accurate acquisition of three-dimensional spatial data, widely applied in remote sensing areas such as surface mapping, environmental monitoring, urban modeling, and forestry inventory. LiDAR remote sensing primarily includes data interpretation and LiDAR-based inversion. However, LiDAR interpretation typically relies on dense and precise annotations, which are costly and time-consuming. Similarly, LiDAR inversion depends on scarce supervisory signals and expensive field surveys for annotations. To address this challenge, weakly supervised learning has gained significant attention in recent years, with many methods emerging to tackle LiDAR remote sensing tasks using incomplete, inaccurate, and inexact annotations, as well as annotations from other domains. Existing review articles treat LiDAR interpretation and inversion as separate tasks. This review, for the first time, adopts a unified weakly supervised learning perspective to systematically examine research on both LiDAR interpretation and inversion. We summarize the latest advancements, provide a comprehensive review of the development and application of weakly supervised techniques in LiDAR remote sensing, and discuss potential future research directions in this field.

Keywords: LiDAR remote sensing, Weakly supervised learning, LiDAR Point clouds, LiDAR Waveform, Ubiquitous annotations

1. Introduction

LiDAR (Light Detection and Ranging) has emerged as a cornerstone of modern remote sensing, offering unparalleled capabilities in capturing high-precision, three-dimensional data of the Earth's surface [1, 2]. Its unique ability to measure distances with high accuracy, penetrate tree canopy, and generate 3D point clouds has driven its adoption across a wide range of applications. From urban modeling and forestry monitoring to ecological and environmental studies, LiDAR's versatility has transformed how we analyze and interpret the physical world. Additionally, it aids various applications, such as mapping terrain under dense vegetation, and facilitating urban management.

From an interdisciplinary perspective, LiDAR remote sensing technology plays a dual role across various application fields: it serves both as a data source that requires interpretation and as a sparse signal that supports large-scale remote sensing inversion. As a data source, LiDAR data is derived from different platforms and sensors, including space-based systems (e.g., ICESat-2), airborne systems (e.g., drones and aircraft), and ground-based systems (e.g., sensors mounted on vehicles or tripods). Its interpretation include denoising [3, 4], filtering [5], registration [6], point cloud segmentation [7, 8], and 3D

reconstruction [9]. On the other hand, LiDAR, as a weak supervisory signal in remote sensing inversion, plays a crucial role, especially when combined with optical data. It is widely applied in large-scale retrieval of surface properties such as forest height, building height, biomass, leaf area index [10], sea ice thickness [11], and snow depth [12], as shown in Fig. 1.

LiDAR interpretation and inversion face several common challenges. Firstly, LiDAR interpretation often relies on a large number of accurate manual annotations, but the high quality of such annotations requires significant time and resources, making the process costly in practical applications [13]. Similarly, LiDAR inversion also encounters high annotation costs. Due to the sparsity of LiDAR data, large-scale, continuous surface mapping is difficult to achieve independently [14]. However, acquiring more annotated data typically necessitates field surveys to measure tree diameter at forest height, tree height, leaf area index, etc., which is time- and resource-intensive [15]. Secondly, both LiDAR interpretation and inversion face domain shift issues [16, 17]. LiDAR data collected from different platforms exhibit significant variations in density, resolution, coverage, and noise levels, leading to notable domain shifts. Additionally, the Earth's surface is diverse and constantly changing, covering various terrains such as cities, forests, mountains, and water bodies, which further exacerbates domain shift problems.

In response to these challenges, weakly supervised learning provides an effective solution [18]. Unlike traditional supervised learning that relies on large amounts of high-quality annotated data, weakly supervised learning combines limited an-

*These authors contributed equally to this work.

**Corresponding author.

Email address: wangcheng@aircas.ac.cn (Cheng Wang)

notated data with unannotated or noisy annotated data, leveraging techniques such as consistency regularization [19], self-training [20], pseudo-labeling [21], active learning [22], and feature alignment [23]. This optimizes the model’s learning process, allowing for more accurate results even in the context of scarce annotations. This approach offers a new perspective for LiDAR data interpretation and inversion and holds promise for addressing issues related to high annotation costs, domain shift, and data sparsity.

However, most researchers have focused solely on LiDAR data interpretation under weak supervision or only on LiDAR-assisted large-scale remote sensing inversion. Few studies have been able to examine LiDAR remote sensing from a unified perspective, considering the dual role of LiDAR. Although several reviews on point clouds have been published, they have certain limitations. The survey in [26] covers a wide range of topics without focusing on LiDAR remote sensing, overlooking reviews in the field of remote sensing inversion. Works like [27, 28] focus on fully supervised learning, neglecting weakly supervised approaches, and [29] provides systematic reviews only on unsupervised learning. In summary, a thorough and comprehensive review of LiDAR remote sensing from the perspective of weak supervision is highly needed and timely.

To the gaps between different research directions and advancing the development of LiDAR remote sensing, this review focuses on two primary aspects: **the interpretation of LiDAR remote sensing data under weak supervision and the use of LiDAR as a weak supervisory signal in remote sensing**, and aims to comprehensively explore the potential and challenges of LiDAR remote sensing in various applications from the perspective of weak supervision. Fig. 2 provides an overview of the entire article. The contributions of this paper are summarized as follows:

- To the best of our knowledge, this is the first review to examine LiDAR remote sensing from a unified perspective, considering its dual role as both a data source and weak supervision signals.
- This paper explores recent advancements in interpreting LiDAR data under weak supervision and utilizing LiDAR as a weak supervisory signal in remote sensing, offering readers state-of-the-art methods.
- This paper highlights promising research directions in LiDAR remote sensing from a weak supervision perspective and explores the potential for integrating more weakly supervised learning techniques into LiDAR-aided inversion.

The structure of this paper is as follows. Section 2 reviews weak supervised interpretation of LiDAR data. Section 3 reviews that LiDAR serves as a weak supervisory signal when combined with optical data. Section 4 discusses our perspectives and reveals possible research directions in the future. Finally, Section 5 concludes the paper.

2. LiDAR Interpretation with Weak Supervision

In LiDAR remote sensing, we deal with massive point cloud data from various sources, such as airborne and space-borne LiDAR. High-precision interpretation of LiDAR data heavily relies on supervised machine learning models, which, in turn, require large volumes of high-quality and densely annotated data. However, acquiring such annotations is costly, particularly in the context of Earth observation, where regional variations, differences in land cover, and temporal changes in these features pose significant challenges to both the accuracy and generalization capability of models. To address this issue, weakly supervised learning methods have gained increasing attention in recent years. These approaches allow for training models with limited or imprecise labels, significantly alleviating the need for extensive annotations. As a result, weakly supervised learning has become a crucial and promising direction for LiDAR data interpretation, offering a path forward in overcoming the limitations of traditional supervision.

Weakly supervised learning in LiDAR remote sensing can be categorized into three types [47]: **Incomplete Supervision**, where only a subset of training data is labeled while the rest remains unlabeled; **Inexact Supervision**, where annotations are coarse-grained, such as providing scene-level labels instead of point-level labels in semantic segmentation; and **Inaccurate Supervision**, where annotation data may contain errors or noise. In addition, there is **domain adaptation** [48], which utilizes the fully labeled data in the source domain and the small amount or unlabeled data in the target domain to improve the task performance in the target domain by reducing the distribution differences between the two domains. Table 1 shows a summary of representative approaches.

2.1. Incomplete supervision

Incomplete supervision addresses the situation in which we are given a tiny portion of the labels as supervised signals and how to use the remaining vast amount of unlabeled data to ensure effective learning in the network [47, 49, 50], as shown in Fig. 3. It consists of two labeling strategies: parts of the point cloud scenes are densely labeled while the remainder are not labeled, and a small number of points are sparingly labeled in point cloud scenes. According to the relevant literature [47], the former is referred to as “semi-supervised learning” [47, 49, 50, 51], and the latter is referred to as “weakly supervised learning with sparse annotations” [52, 53, 54, 55].

2.1.1. Semi-supervised learning

It aims to improve network learning performance by utilizing a small portion of fully labeled training data from the scene and a large portion of unlabeled scene data [47, 49, 50, 51]. A lot of research has been done about the point cloud field, such as contrastive learning [56], consistency regularization [57], pseudo-label [58, 59], self-training [20], etc.

Semi-supervised 3D semantic segmentation is to completely utilize the data, with certain scenes fully labeled and the majority of the remaining scenes unlabeled, in order to achieve semantic annotation of all data. Li *et al.* [20] uses a self-training

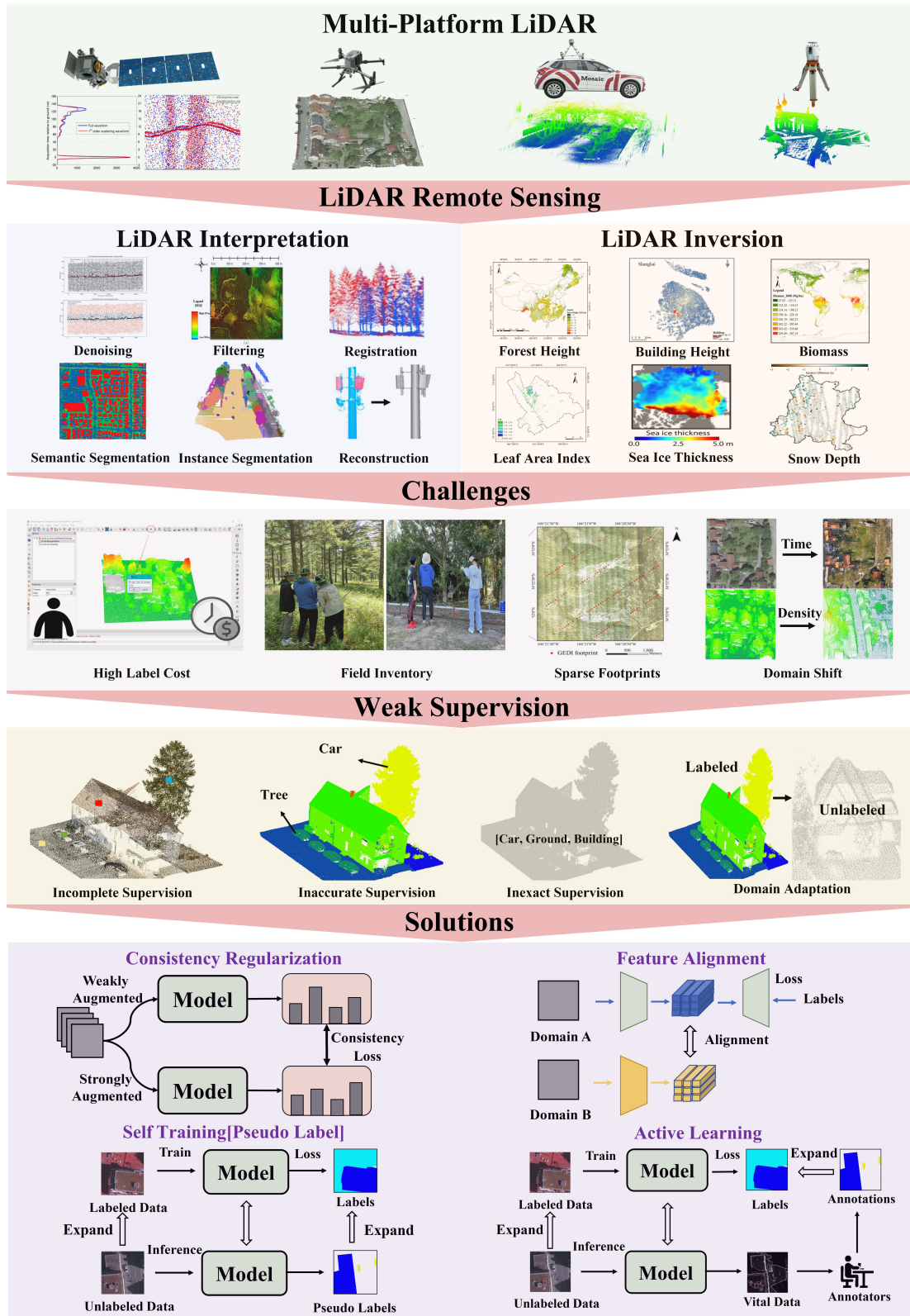


Figure 1: An overview of LiDAR remote sensing meets weak supervision. LiDAR remote sensing data are primarily obtained from satellite, airborne, vehicle-mounted, and ground-based platforms, providing rich surface information. The interpretation tasks for LiDAR data include denoising, filtering, registration, semantic segmentation, instance segmentation, and 3D reconstruction. Inversion tasks involve estimating forest height, building height, biomass, leaf area index, sea ice thickness, and snow depth. These tasks face challenges such as high annotation costs, domain shift, difficulties in field validation, and sparse supervisory signals. To address these challenges, weakly supervised learning techniques such as incomplete, inaccurate, inexact supervision, and domain adaptation can be employed. Additionally, methods like consistency regularization, pseudo-labeling, self-training, active learning, and feature alignment can effectively improve model generalization. These images are obtained from [2, 4, 24, 8, 10, 12, 11, 7, 5, 6, 9, 25].

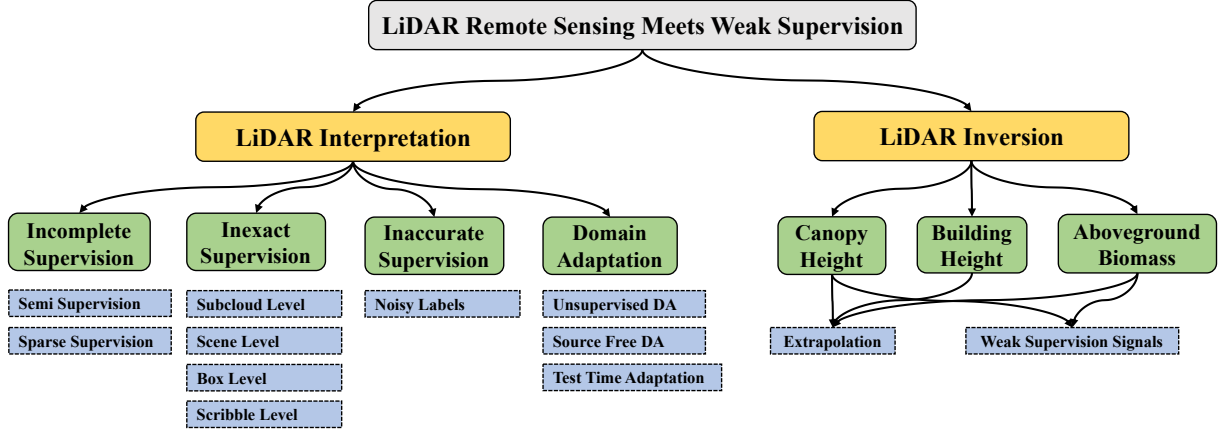


Figure 2: A taxonomy of methods and applications for LiDAR remote sensing meets weak supervision. LiDAR interpretation is primarily divided into incomplete supervision, inexact supervision, inaccurate supervision, and domain adaptation. Based on related literature, these tasks can further be categorized into semi-supervision, sparse supervision, scene-level supervision, noisy labels, unsupervised domain adaptation, and others. For LiDAR inversion, from an application perspective, they are mainly classified into canopy height, building height, and above-ground biomass estimation. Technically, inversion methods are divided into generalization approaches and the use of LiDAR as a weak supervision signal.

Table 1: Representative works of LiDAR remote sensing interpretation with weak supervision.

Weak supervision	Setting	Task	Method	Contribution
Incomplete Supervision	Semi supervision	Semantic segmentation	SSGF[30] Li et al. [31] TSDN [32] UF2SCN [33] SMDN [34] Dersch et al. [35]	Handle labeled and unlabeled data via graphs separately Enhance intra-class information interaction via contrastive learning Generate high-confidence pseudo-labels using superpixel segmentation and multiview prediction results Improve the complementarity of HSI and LiDAR data via a one-way transmission structure Guide feature training in a subspace with limited labeled samples Generate tree labels by pre-clustering LiDAR point clouds using NCut
		Object detection	-	-
		Instance segmentation	-	-
	Sparse supervision	Semantic segmentation	Wang et al. [36] Wang et al. [18] WSPointNet [37] DAAL-WS [38]	Select reliable pseudo-label via adaptive thresholding Penalize class overlap in predictive probabilities via entropy regularization Provide adaptive supervision through a pseudo-label branch Select critical labeling points via active learning
Object detection		-	-	
Inexact Supervision	Box level supervision	-	-	-
	Subcloud level supervision	Semantic segmentation	Lin et al. [39]	Explore semantic information between adjacent subclouds through overlap region loss
	Scene level supervision	Semantic segmentation	Wang et al. [40]	Select informative subclouds for annotation using TOD-based active learning
	Scribble level supervision	-	-	-
Inaccurate Supervision	Noisy label supervision	Semantic segmentation	ADNLC [41]	Help the network learn true labels by iteratively updating noisy labels
Domain Adaptation	Unsupervised domain adaptation	Semantic segmentation	Luo et al. [23] Peng et al. [42] Xie et al. [43] SegTrans [44] Wang et al. [45] PS-UDA [46]	Align source and target domain feature distributions using an MCD-based adversarial framework Achieve point feature and global feature alignment through adversarial training Reduce cross-city domain shift via appropriate point cloud density and suitable data augmentation methods Align feature distributions of source and target domains using adversarial learning Reduce domain gaps using alignment, normalization, enhancement, and weighted cross-entropy Train the target domain GCN classifier using enhanced target domain features and high-quality pseudo-labels
		Source free domain adaptation	-	-
		Test time adaptation	Semantic segmentation	Yao et al. [16]
	-	-	-	-

paradigm to improve the segmentation performance. [58, 59] generate pseudo-labels for unlabeled point clouds. Zhang *et al.* [57] utilizes consistent prediction of the teacher model and the student model to improve the performance of the segmentation network. Jiang *et al.* [56] apply contrast learning to 3D point cloud semantic segmentation. Some research [60, 56, 61, 62] applies semi-supervised learning for LiDAR semantic segmen-

tation in autonomous driving. For instance, LaserMix [60] mixes laser beams from different LiDAR scans by exploiting a priori knowledge of spatial cues and maintains consistent prediction of the segmentation network before and after mixing.

In **LiDAR remote sensing**, most research focuses on airborne LiDAR point clouds. For instance, Liao *et al.* [30] propose a semi-supervised graph fusion framework to fuse spectral, spatial, and elevation features of LiDAR and hyperspectral data. Li *et al.* [31] propose a two-stage classification method with pseudo-label contrast learning to solve the time-consuming and laborious problem of jointly classifying labeled samples with HSI and LiDAR. Li *et al.* [32] generate high-confidence pseudo-labels using a novel label calibration module to enhance semi-supervised learning. Guo *et al.* [33] first extract fused features from all samples and then classify them using a limited number of labeled samples. Pu *et al.* [34] employ an unsupervised encoder-decoder structure combined with a data-specific branch to perform joint training, enabling the extraction of effective multimodal representations even with lim-

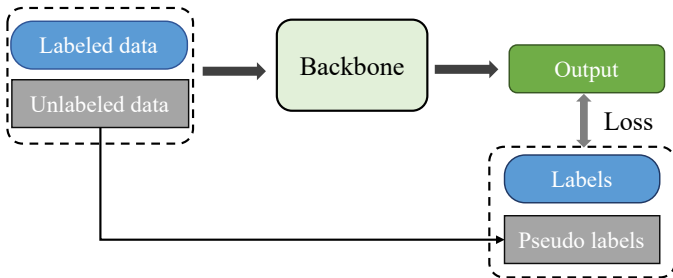


Figure 3: Incomplete supervised learning framework for point clouds.

ited labeled samples. Additionally, Dersch *et al.* [35] utilize semi-supervised learning for multi-class tree crown delineation.

Multi-source data fusion is increasingly favored in LiDAR remote sensing for information complementarity. Combining hyperspectral and LiDAR data addresses their individual shortcomings: hyperspectral’s susceptibility to SODS/SSDO hinders accurate classification, while LiDAR lacks object detail. Fused data provides comprehensive, mutually reinforcing surface information, boosting classification accuracy and robustness significantly.

Semi-supervised 3D object detection is the task of estimating object classes and 3D bounding boxes for all objects in a scene using labeled and unlabeled data. It can be divided into two groups: consistency-based methods [63] and pseudo-labeling methods [21].

Zhao *et al.* [64] propose a robust 3D object detector trained via the Mean Teacher paradigm, incorporating point cloud-specific perturbations and consistency loss. Similarly, Wang *et al.* [65] utilize a teacher-student mutual learning framework to propagate information from labeled data to unlabeled data in the form of pseudo-labels. Outdoor LiDAR point clouds present unique challenges such as complex structures [60] and low point density [66]. Research on 3D point cloud object detection in LiDAR remote sensing is limited. Current research [65, 67, 68, 69, 70, 71, 72, 73] is largely focused on LiDAR point clouds for autonomous driving. For instance, 3DIoUMatch [65] set a milestone in semi-supervised 3D object detection by creating a novel pseudo-label filtering method guided by both detection scores and IoU. Qi *et al.* [67] leverage temporal points through multi-frame object detection to achieve an offboard 3D object detection pipeline. Xu *et al.* [68] generate high-quality pseudo-labels through an adaptive class confidence selection module and utilize a holistic point cloud augmentation module to improve robustness. Wong [73] takes into account the non-coincidence and weak correlation of the target objects in the point cloud by introducing two mechanisms: strict thresholding and filter switching, to realize that only the truth-determining pseudo labels are retained and the other fuzzy labels are pruned.

Semi-supervised 3D instance segmentation combines a small amount of labeled data with a large amount of unlabeled data to achieve semantic classification and instance differentiation of objects in point clouds, aiming to reduce annotation costs and improve model performance.

Compared to semi-supervised 3D semantic segmentation and object detection, research on semi-supervised 3D instance segmentation is limited [74, 75, 76, 77]. For instance, Liao *et al.* [74] force the predictions of different perturbations of the input point cloud to remain constant to achieve semi-supervised point cloud instance segmentation. Chu *et al.* [76] use pseudo semantic labels and pseudo offset vectors for semantic and instance-level supervision, with an object-level denoising module and a bidirectional mutual enhancement mechanism to iteratively improve pseudo label quality. Liu *et al.* [77] apply a contrast learning strategy to guide multi-stage network training.

2.1.2. Sparse-supervised learning

It refers to the scenario in 3D point cloud data where only a small number of points are sparsely labeled, and these limited annotations, combined with large amounts of unlabeled data, are used to train the network effectively. The research methods include consistency regularization [19, 78], contrastive learning [79], self-training [80], label propagation [52, 81], pseudo-label [36, 37, 81, 82], active learning [22, 80], and others.

Sparse-supervised 3D semantic segmentation refers to performing semantic segmentation on 3D point cloud data where only a subset of points are labeled, while most remain unlabeled. The goal is to train a model capable of accurately segmenting the entire point cloud using limited labeled information.

A large number of well-established works [19, 52, 78, 83, 22, 84, 85] have emerged. Xu *et al.* [19] employ a teacher-student model and leverage active learning to select and label the most informative samples, achieving good results with very little labeled data. Considering information redundancy in existing active learning strategies, Xu *et al.* [22] design a feature distance suppression module to select the important points to be labeled. Liu *et al.* [52] label one point for each object and propagate the labels to unknown regions through a graph propagation module. [78, 83] force predictive consistency of the original and perturbation branches. Hu *et al.* [84] leverage the semantic similarity of neighboring 3D point clouds by encoding raw point clouds and their neighbors into vectors to predict semantic labels. [86, 80, 81, 82, 87, 88] apply similar strategies like pseudo-labeling, active learning, and self-training to LiDAR point clouds in autonomous driving. For instance, Hu *et al.* [80] propose a new active learning strategy for 3D LiDAR semantic segmentation based on the inconsistency of inter-frame prediction to estimate model uncertainty and further ensemble self-training to further improve performance. Zhao *et al.* [81] propagate pseudo-labels between adjacent frames and select reliable labels for learning.

Currently, there is very limited research on **LiDAR remote sensing**. For *airborne laser point cloud*, Wang *et al.* [36] propose a pseudo-label-assisted point cloud segmentation method, which generates pseudo-labels by setting an adaptive threshold for the prediction results of unlabeled data, after which the pseudo-labels are used for iterative training. In addition, they penalize the uncertainty in the prediction class by introducing entropy regularization while imposing consistency constraints between the predictions and the integrated predictions to improve the robustness of the network [18]. For *mobile laser point cloud*, Lei *et al.* [37] propose a multi-branch weakly supervised learning network (WSPointNet), which contains an integrated prediction constraint branch to improve the stability of point cloud prediction, a contrast-guided entropy regularization branch to prevent model overfitting, and an adaptive pseudo-label learning branch. Subsequently, they propose a novel weakly supervised MLS point cloud semantic segmentation method by incorporating data augmentation and active learning strategies into WSPointNet [38].

Sparse-supervised 3D object detection refers to detecting

objects in 3D point clouds, where only a subset of objects are labeled while most remain unlabeled. The task involves predicting the object categories and their corresponding 3D bounding boxes. Most research is focused on LiDAR point clouds for autonomous driving, with fewer studies targeting indoor point clouds and virtually none addressing LiDAR remote sensing.

Xu et al. [89] implement a weakly supervised object detection method for indoor point clouds by using synthesized 3D shapes to convert weak labels into fully annotated virtual scenes as stronger supervision. For LiDAR Point Cloud in autonomous driving, Liu et al. [54] mine positive instances through a missing-annotated instance mining module and design a reliable background mining module and a point cloud filling data augmentation strategy to generate confidence data for iterative learning. Meng et al. [90] utilize a small number of weakly annotated scenarios to generate cylindrical object proposals and refine cylindrical proposals using a small number of accurately labeled object instances to obtain cuboids and confidence scores. Xia et al. [91] enhance feature recognition by introducing a multi-class contrast learning module (MCcont) and supervise detector training with the introduction of an instance feature mining module and a mark-to-pseudo contrast learning module. Considering that existing weakly supervised and semi-supervised methods are difficult to adapt to different scenarios (e.g., indoor or outdoor), Zhang et al. [92] utilize a small amount of full box-level annotations and a large amount of point-level annotations to generate high-quality pseudo-boundary boxes for training any 3D detector by modeling the global interactions between the LiDAR points and the corresponding weak labels. Yang et al. [93] utilize a large number of coarse cluster-level labels to learn semantics and a number of expensive box-level labels to learn accurate poses and shapes. Gao et al. [94] improve PointDETR [95] and propose PointDETR3D, a faculty-student framework for weakly supervised 3D detection.

Sparse-supervised 3D instance segmentation refers to performing instance-level segmentation on 3D point cloud data where only a subset of points or instances are labeled. The goal is to assign each point to a specific instance ID while predicting the instance’s category label.

Hou et al. [96] observe that PointContrast [97] uses a simple pretext task based on contrast learning that focuses only on point-level correspondence matching and propose a method to integrate spatial information into the contrast learning frame. Tao et al. [98] transform instance location annotations into segment-level labels via oversegmentation and then generate point-level pseudo-labels from these using a segment grouping network (SegGroup). Tang et al. [99] extend point-level labels to the superpoint level and leverage inter-point affinities to generate high-quality pseudo-labels. Liu et al. [100] annotate one point for each instance and further devise a new similarity metric for clustering to generate pseudo-labels. Dong et al. [101] propose a weakly supervised 3D instance segmentation method that only requires categorical semantic labels and not instance-level labels as supervision. They propagate semantic and instance information to unknown regions by self-attention and cross-graph random wandering, respectively [102].

2.2. Inexact supervision

Inexact supervision refers to providing coarse-grained labels instead of precise point-wise annotations. The goal is to train a model using rough labeling information to achieve accurate point-level tasks. It typically includes sub-cloud-level annotations [103, 104, 39], scribble annotations [105], bounding box annotations [104, 106, 107, 108, 109, 110, 111, 112], and scene-level annotations [113, 13], among others.



Figure 4: Bounding box annotations (left) and point-wise semantic labels (right) from the H3D dataset [24].

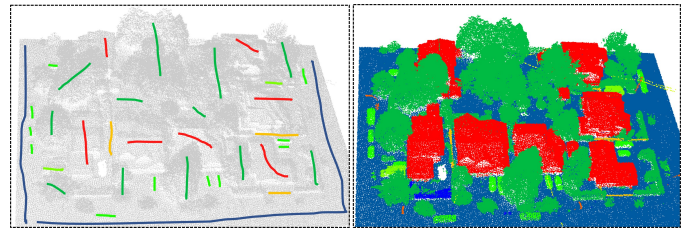


Figure 5: Illustration of scribble-labeled LiDAR point cloud scenes (left) and corresponding overlaid frames (right) from the DALES dataset [7].

3D semantic segmentation. Liu et al. [104] utilize *box-level annotations*, as shown in Fig. 4, and combine them with self-training and point activation maps to reduce the cost of point-wise labeling. Unal et al. [105] use *scribbles* to annotate LiDAR point clouds, as shown in Fig. 5, which also significantly improves the efficiency of point cloud annotation. Some studies [104, 103, 39] use *subcloud-level* labels to reduce annotation costs, assigning the classes present within the sampled regions as labels. For instance, Wei et al. [103] propose a point cloud scene segmentation network from cloud-level weak labels on indoor 3D data, and they introduce a multipath region mining module. Lin et al. [39] propose a weakly supervised semantic segmentation method for **airborne laser scanning (ALS) point clouds**. They leverage weak subcloud annotations, as shown in Fig. 6, first generating accurate pseudo-labels using a classification network with overlap region loss and elevation attention, and then optimizing a segmentation network with supervised contrastive loss to efficiently learn from limited subcloud labels. Compared to the above labeling methods, more studies prefer using *scene-level* labels [113, 53, 114, 40, 13, 115, 116, 98], where only the class information of the entire scene is provided for 3D point clouds, without annotating individual points or object instances, as shown in Fig. 7. For instance, Ren et al. [113] introduce scene-level annotations as supervision while addressing point-level semantic segmentation, 3D proposal generation,

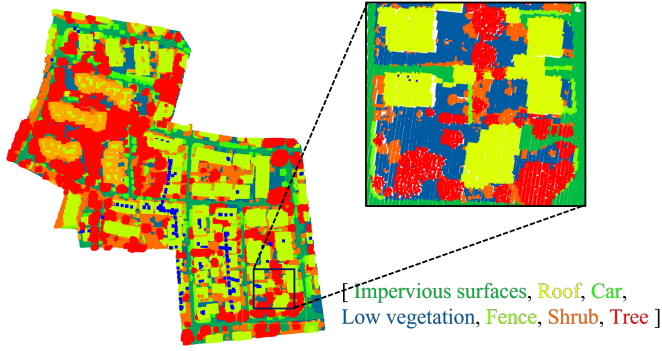


Figure 6: Example of subcloud-level annotated point cloud from the ISPRS dataset [117].

and 3D object detection, achieving better results than previous methods. Xia *et al.* [13] achieve recent performance of fully supervised methods using scene-level annotations propagated to each point and conservative methods for creating pseudo-labels.

In **LiDAR Remote Sensing**, Wang *et al.* [40] train by assign-

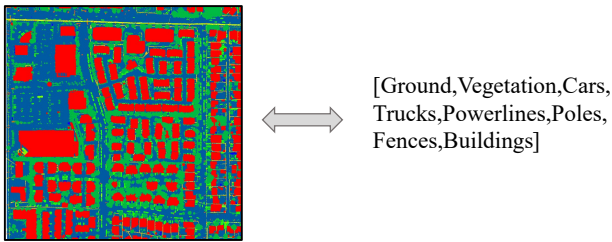


Figure 7: Example of scene-level annotated point cloud from the DALES dataset [7].

ing a point to each class label of the sub-cloud, incorporating contextual constraints and pseudo-label generation. They use active learning based on Temporal Output Discrepancy (TOD) to select the most informative sub-point clouds for labeling, achieving near fully-supervised segmentation performance with minimal labeled data on ALS, MLS, and TLS datasets.

3D object detection. Some studies use *position-level* annotations [118, 89] instead of 3D bounding boxes for 3D object detection to reduce annotation costs. For instance, Meng *et al.* [118] combine bird’s-eye view (BEV) center-click annotations with a small number of precise 3D instance labels to significantly reduce annotation costs. Scene-level annotation is a simpler approach. WyPR [113] uses simple scene-level labels and addresses the problem of weakly supervised 3D point cloud object detection through multi-task learning and self-supervised constraints. Qin *et al.* [119] combine scene-level labels with results from a pre-trained network applied to images mapped from 3D point clouds as soft labels, significantly reducing annotation costs while maintaining 3D object detection performance. Wei *et al.* [120] use 2D bounding box annotations to train a 3D object detector without relying on precise 3D labels.

3D instance segmentation. Some research [106, 108, 107, 109, 110, 111, 112] uses *box annotations* to reduce labeling costs. For instance, GaPro [107] generates pseudo-labeled masks from 3D bounding boxes to train a 3D point cloud in-

stance segmentation network. Box2Mask [109] replaces dense point-level annotations with 3D bounding box labels, leveraging a voting mechanism and non-maximum clustering to effectively address 3D instance segmentation under weak supervision.

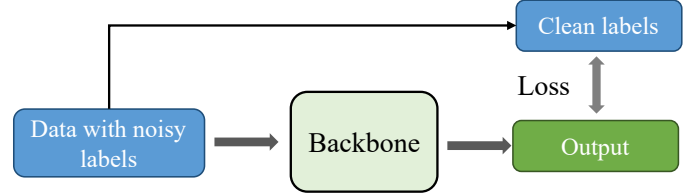


Figure 8: Inaccurate supervised learning framework for point clouds.

2.3. Inaccurate supervision

Inaccurate supervision refers to cases where labels contain errors or noise, causing the supervision signal to deviate from the true information, as shown in Fig. 8. Techniques such as sample selection [121, 122] and label correction [123] can mitigate the negative impact of inaccurate labels on model training and improve performance.

Research on robust learning with noisy labels in point clouds is limited. Ye *et al.* [124] propose the novel Point Noise Adaptive Learning (PNAL) framework, which uses point-by-point confidence of historical predictions for each point to select reliable labels and considers neighborhood correlation to generate the best labels using a voting strategy. Chen *et al.* [125] consider the paradigm of teacher-student models and design a noise-resistant instance supervision module to eliminate the negative effects of noisy labels from a noise learning perspective. Gao *et al.* [41] propose a new semantic segmentation framework for handling **airborne LiDAR point cloud** data with noisy labels, which adaptively corrects noisy labels based on the learning state of different categories to enhance the network’s robustness against noise.

In recent years, 2D *foundation models* like Contrastive Vision-Language Pre-training (CLIP) [126] and Segment Anything (SAM) [127] have achieved significant success in 2D vision tasks. These models are typically pre-trained on large-scale datasets and then fine-tuned for specific tasks, often outperforming traditional methods. Some studies [128, 129, 130, 131, 132] have applied these powerful 2D foundation models to 3D tasks, enhancing the performance of 3D scene understanding. *Pseudo-label.* This method uses a foundation model to segment the projected image of the point cloud and then maps the segmentation result back to the point cloud through reprojection or other methods to obtain pseudo-labels [133, 134, 135, 88, 136, 137, 138, 139, 140, 141]. For instance, Segment3D [133] uses high-quality segmentation masks generated by the 2D foundation model SAM to automatically generate labels for point clouds, instead of manual annotations. Dong *et al.* [134] utilize sparse 2D point annotations as prompts, project 2D semantic segmentation results into 3D space, and combine pseudo-labels from different viewpoints using a voting strategy to generate high-quality 3D semantic pseudo-labels. *feature alignment.* Chen *et al.* [142] utilize SAM generates

semantic masks from 2D images, which are projected onto 3D point clouds for region-level segmentation and 2D-3D alignment. Dense feature distillation is then applied to transfer 2D features to 3D point clouds.

Table 2: Domain adaptation settings.

Setting	Data		Learning	
	Source	Target	Train stage	Test stage
Domain adaptation	x^s, y^s	x^t, y^t	Yes	No
Unsupervised domain adaptation	x^s, y^s	x^t	Yes	No
Source free domain adaptation	-	x^t	Yes	No
Test-time adaptation	-	x^t	No (pre-trained)	Yes
Continual test-time adaptation	-	x^t	No (pre-trained)	Yes

2.4. Domain adaptation

The methods described above are primarily designed for a single domain, where applying a pre-trained model to the same domain achieves optimal results. However, remote sensing data is highly affected by temporal, seasonal, and regional variations, leading to domain shift in the acquired LiDAR data. This issue is further amplified by the use of different sensor platforms (e.g., ALS, TLS, MLS), causing a performance decline when pre-trained models are applied to shifted domains.

To address this issue, “**domain adaptation**” aims to transfer knowledge from a labeled source domain to an unlabeled target domain, thereby reducing annotation costs and mitigating the effects of domain shift. It can be regarded as an effective weakly supervised learning approach, as it does not require labeled data from the target domain, offering a practical solution to the challenges of expensive and time-intensive annotation. It includes unsupervised domain adaptation, source free domain adaptation, (continual) test time adaptation, and so on. Their differences are shown in Table 2.

2.4.1. Unsupervised domain adaptation

Unsupervised Domain Adaptation (UDA) aims to leverage a labeled source domain model to improve performance on an unlabeled target domain. The main challenge is to transfer domain-invariant features from the source to the target domain. Most UDA research has focused on 2D images [143, 144, 145, 146, 144, 147], with only a few studies addressing 3D point clouds. Several approaches have been proposed to tackle the unsupervised domain adaptation problem for 3D point clouds, including adversarial learning, self-training, feature alignment, and so on.

PointDAN [148] is the first work to address point cloud classification in the UDA context, which leverages local and global feature modeling to extract multi-scale information and employs adversarial training to minimize the distribution discrepancy between the source and target domains. Following PointDan, these studies [149, 150, 151, 152, 153] also adopt the adversarial learning strategy to solve the 3D UDA problem. Achituve et al. [154] propose a novel approach for domain adaptation on point clouds by combining the *self-supervised* task of Deformation Reconstruction (DefRec) with Point Cloud Mixup (PCM). DefRec simulates local deformations of point clouds

and reconstructs the original shapes, enabling the model to learn cross-domain geometric and semantic features. PCM enhances generalization by generating new training samples through random sampling and mixing of point clouds. [155, 156] also apply self-supervised learning to UDA tasks.

Self-training is another line for this task, which leverages pseudo-labels to learn target knowledge gradually. Cardace et al. [157] propose the RefRec method, which leverages shape reconstruction tasks to learn global shape descriptors for refining pseudo-labels. Combined with self-training strategies and domain-specific classification heads, the method effectively mitigates domain discrepancies, enhancing the performance of unsupervised domain adaptation for point cloud classification. [158, 159, 160, 161, 162, 163, 164] based self-training mechanisms have achieved SOTA performance in the field of 3D UDA.

Additionally, some methods [165, 166, 167, 168, 169] adopt *feature alignment* strategies. Wang et al. [169] address the complex domain discrepancies in indoor synthetic-to-real 3D object detection using object-aware augmentation, hierarchical domain alignment (class-level and holistic-level), and pseudo-label optimization strategies.

In recent years, with the rapid development of *foundation models*, some studies [170, 171, 172] have integrated them to address point cloud UDA tasks. Peng et al. [170] leverage the 2D image embeddings provided by the Segment Anything Model (SAM) as a bridge to align 3D point cloud features from different domains into a unified feature space. Wu et al. [171] utilize the vision-language knowledge of the CLIP model to generate task-specific text embeddings through Visual-driven Prompt Adaptation (VisPA) and achieve multi-modal feature fusion via Text-guided Context Interaction (TexCI). Xu et al. [172] leverage the knowledge priors of Visual Foundation Models (VFMs) to generate high-precision pseudo labels (VFM-PL) and employ a FrustumMixing strategy to semantically mix source and target domain data, reducing distribution discrepancies.

However, research on point cloud UDA in the **LiDAR remote sensing** domain remains limited. [23, 42, 43, 44, 45, 46] apply the same method: feature alignment. For instance, Luo et al. [23] effectively improve cross-scene MLS point cloud semantic segmentation performance through adaptive data and feature alignment on the target domain point cloud. Peng et al. [42] align local geometric features and global features and reduce the distribution discrepancy between source and target domains through adversarial training. Xie et al. [43] enhance the model generalization through data augmentation techniques and introduce the Deep CORAL method, which aligns second-order statistics of features to achieve cross-city semantic segmentation of ALS point clouds. Shen et al. [44] alleviate the data domain gap by selecting similar scenes based on the scene height distribution, and align the feature distributions using the adversarial learning module (ALM) solving the domain adaptation problem from terrestrial laser scanning (TLS) data to mobile laser scanning (MLS) data.

2.4.2. Source free domain adaptation

Traditional domain adaptation (DA) requires simultaneous access to both source domain data and target domain data for model adaptation. In contrast, source-free domain adaptation (SFDA) [173, 174, 175, 176, 177, 178] relies solely on a pre-trained model from the source domain and performs adaptation to the target domain without access to source domain data. This is achieved by leveraging unlabeled target domain data and utilizing pseudo-labels or feature distributions generated by the model to update its parameters for improved performance in the target domain.

Currently, SFDA is predominantly focused on 2D image processing, while research in 3D point clouds remains relatively limited. [165, 179, 180, 181] apply pseudo-label to solve SFDA. For instance, Saltori et al. [165] propose the first source-free unsupervised domain adaptation framework for LiDAR-based 3D object detection. Wang et al. [180] employ pseudo-label optimization and prototype matching to achieve point cloud primitive segmentation under the source-free domain adaptation paradigm. In contrast to their approach, Tian et al. [182] utilize a Gaussian Mixture Model (GMM) to generate virtual domain samples and enhance the intra-class compactness of the target domain to achieve effective alignment between the target and virtual domains.

2.4.3. Test time adaptation

Test-Time Adaptation (TTA) refers to the process of dynamically optimizing a model during the testing phase using unlabeled target domain data to address domain shift, without accessing source domain data or ground-truth labels. Continual Test-Time Adaptation (CTTA) extends TTA by enabling the model to progressively adapt to continuously changing target domains while retaining its adaptability to previous data distributions, making it suitable for more complex and dynamic scenarios. Most (C)TTA methods are currently applied to 2D images, including techniques such as batch normalization calibration [183, 184], entropy minimization [185, 186], contrastive learning [187, 188], and pseudo-labeling [189, 188].

Research on TTA for 3D point clouds remains relatively limited, which is mainly based on pseudo-labeling technology combined with other techniques [190, 191, 179, 192]. For instance, Cao et al. [191] achieve dynamic adaptation to the target domain through single-modal pseudo-label aggregation, cross-modal pseudo-label fusion, and class-wise momentum queue updates. Saltori et al. [179] enhance pseudo-label coverage through adaptive selection and geometric feature propagation while leveraging temporal consistency regularization to enforce feature smoothness across consecutive frames. Research on TTA is also included in other fields such as point cloud classification [193], registration [194, 195], super-resolution [196], and so on.

For **LiDAR remote sensing**, Wang et al. [16] propose a Progressive Batch Normalization (PBN) method. PBN incrementally updates BN layers by integrating statistical information from test batches while optimizing learnable BN parameters through information maximization and pseudo-label generation. Experiments are conducted across three adaptation

scenarios (e.g., photogrammetric to airborne LiDAR, airborne to mobile LiDAR, and synthetic to mobile LiDAR data) and demonstrate the effectiveness of the method on multiple public datasets.

2.5. Summary and discussion

Weak supervision refers to training models using incomplete, imprecise, inaccurate labels, or labels from other domains. This approach provides efficient and labor-saving support for LiDAR data interpretation. Current research mainly focuses on sparse and semi-supervised learning, with notable progress in semantic segmentation, achieving performance comparable to fully supervised models. However, progress in tasks such as object detection and instance segmentation has been more limited. Moreover, while there has been some research on imprecise or inaccurate supervision methods, significant gaps remain, leading to the wastage of extensive labeled data (e.g., crowdsourced labels). With the development of foundation models, this issue is expected to be alleviated. Foundation models can automatically generate labels for LiDAR point cloud data, reducing reliance on manual annotation and significantly lowering labeling costs.

3. LiDAR Inversion with Weak Supervision

In LiDAR remote sensing, LiDAR point clouds are often combined with remote sensing images for large-scale inversion tasks (e.g., canopy height, building height, biomass). Optical imagery provides continuous surface coverage with high revisit frequency and rich spectral information, while LiDAR data serves as supervisory signals, capturing structural and elevation details. However, due to the sparsity of LiDAR data, it cannot cover all inversion areas, making the generation of large-scale continuous maps challenging. Field surveys, which collect data such as tree diameter, height, and leaf area index by setting sampling points and survey regions, can provide more supervision signals but are costly and resource-intensive. Additionally, regional differences and temporal variations can lead to domain shifts, which pose significant challenges to model accuracy and generalization. Weakly supervised learning is an effective approach to reduce costs and enhance model generalization. Current weakly supervised LiDAR inversion primarily includes generalized methods and using LiDAR as weak supervision signals. However, the application of other weak supervision techniques remains limited, and the methods are relatively simple.

In this section, we will review and summarize existing related work. We categorize the applications in LiDAR remote sensing into specific areas, including canopy height mapping, building height estimation, and biomass estimation, as shown in Fig. 9.

3.1. Canopy height estimation

Canopy height is a crucial parameter in forest ecosystems, playing a key role in assessing carbon storage, monitoring ecosystem health, and tracking land-use changes, as shown in Fig. 10. Accurate measurement of canopy height supports scientific research and informs forest management and conservation policies. Traditional ground-based measurements, such as

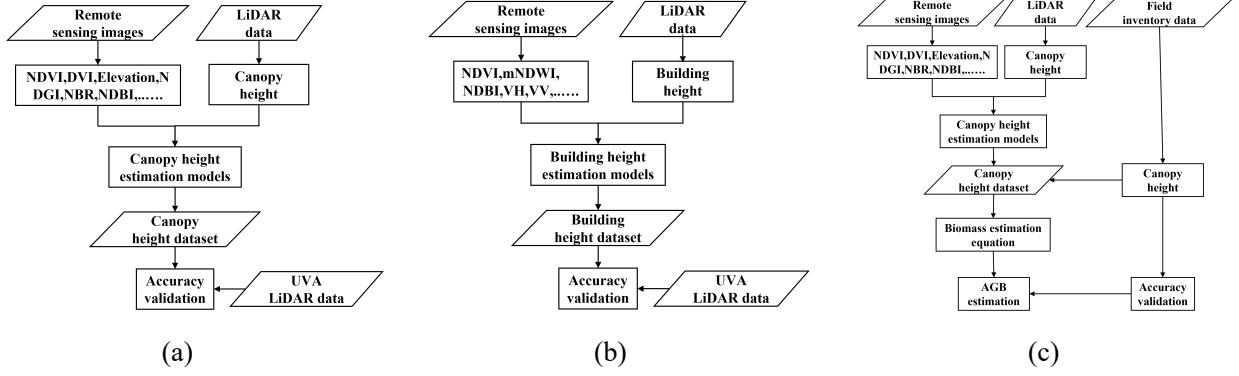


Figure 9: Workflow of LiDAR inversion with weak supervision. (a) canopy height estimation, (b) building height estimation, and (c) biomass estimation.

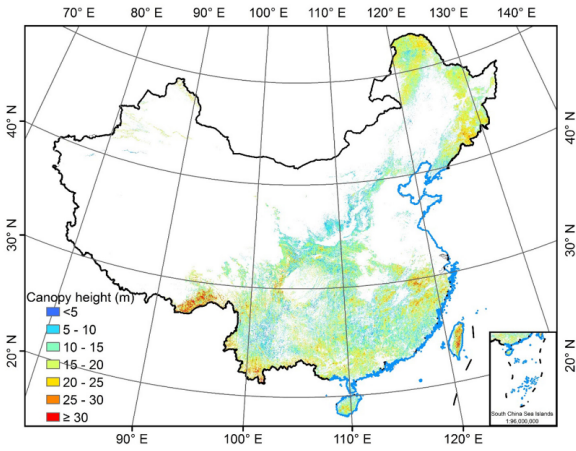


Figure 10: The NNGI-derived forest canopy height of China at 30 m resolution for 2019. The image is obtained from [197].

forest inventories, offer high accuracy but are limited in coverage, time-consuming, and unsuitable for large-scale applications. Satellite remote sensing provides extensive coverage. However, traditional multispectral and high-resolution imagery lacks the capability to capture 3D structural information like canopy height. LiDAR offers precise 3D structural data, but terrestrial and airborne LiDAR have limited spatial coverage. Spaceborne LiDAR, such as GEDI and ICESat, offers global coverage, high data collection efficiency, low cost, and strong temporal consistency while providing high-precision 3D forest structural information [200]. Fig. 11 illustrates how key ecological and terrain information is extracted from GEDI waveforms.

Current methods for canopy height inversion primarily use remote sensing images as training data and point clouds as supervisory signals. One approach involves training in small regions and extrapolating to large-scale areas, as shown in Fig. 12. They train a model using drone lidar data as labels and GEDI/ICESat-2 lidar footprints with environmental auxiliaries as inputs, then apply the trained model across mainland China to produce a high-precision forest canopy height map. Another uses point clouds as weak supervisory signals to directly train on large-scale remote sensing images, yielding large-scale in-

version results, as shown in Fig. 13. Their CNN model uses Sentinel-2 (S2) imagery and encoded geographic coordinates (latitude, longitude) as input, supervised by sparse GEDI LiDAR labels, to estimate dense canopy height and its predictive uncertainty (variance).

Extrapolation. In the early stages, airborne point clouds are often used as weak supervisory signals. For instance, Pourshamsi et al. [201] combine Polarimetric Synthetic Aperture Radar (PolSAR) parameters with limited airborne LiDAR data, using various machine learning algorithms to train on a subset of LiDAR samples and predict forest height over larger areas. The emergence of spaceborne LiDAR has brought new opportunities. [202, 203, 204, 197, 205, 206, 207, 208, 209] use ICESat-2 or GEDI data as supervisory signals and apply machine learning or deep learning to train on remote sensing images, ultimately mapping canopy height. For instance, Potapov et al. [204] integrate NASA GEDI LiDAR data with Landsat multispectral time series data and use a machine learning regression tree model to train a forest canopy height prediction model within the limited coverage of GEDI. They extend the model to a global scale, generating a 30-meter resolution global forest canopy height map for the year 2019. Liu et al. [197] integrate GEDI and ICESat-2 ATLAS data to map the spatially continuous distribution of forest canopy height in China. This method uses drone-lidar data as training samples, trains the model on small regional areas, and then applies the model across the entire country to generate a 30-meter resolution forest canopy height map. Wang et al. [207] combine GEDI LiDAR data with other remote sensing data to improve the estimation of wall-to-wall canopy height.

Deep learning techniques have made groundbreaking progress in recent years in 2D image processing, providing new solutions for the analysis of remote sensing data. Many studies [14, 210, 211, 212] now focus on using deep learning to treat point clouds as **weak supervision signals** for training on large-scale data such as remote sensing images. For instance, Weber et al. [210] propose a unified deep learning-based model to predict global above-ground biomass density (AGBD), canopy height (CH), and canopy cover (CC) by fusing 13-channel inputs from Sentinel-1 and Sentinel-2 satellite imagery, multispectral data, and digital elevation models (DEMs). Fan et

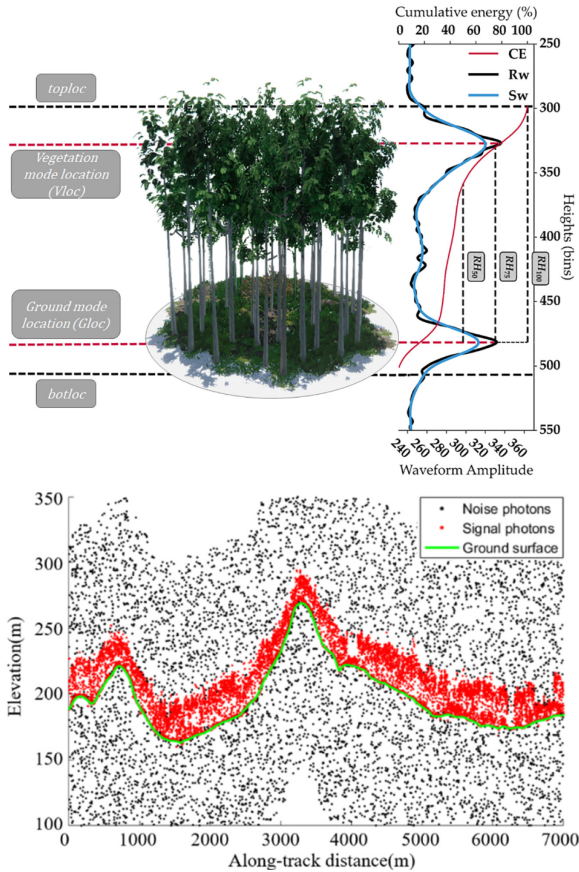


Figure 11: Example of an acquired GEDI waveform (Rw) over an Eucalyptus stand ($H_{dom} = 25.9$ m; $V = 230.7$ m³.ha⁻¹), its smoothing (Sw) and corresponding waveform metrics (top). Strong beams of ICESat-2 in the daytime (bottom). These images are obtained from [198, 199].

al. [211] utilize a customized PRFXception neural network incorporating receptive fields at different scales, which learns canopy height information from sparse LiDAR sampling points and makes continuous inferences over the entire image coverage area, resulting in canopy height estimation at 10 m resolution. Fayad et al. [212] propose a hybrid visual transformer model called Hy-TeC to generate high-resolution tree canopy height maps using multi-source remote sensing data (Sentinel-1 and Sentinel-2) as inputs and GEDI LiDAR data as sparsely supervised ground truth. The model employs an architecture that combines a transformer encoder with a convolutional decoder, combined with a dual loss function of classification and regression to enhance the accuracy of the height intervals.

3.2. Building height estimation

Building height, as a key parameter of urban three-dimensional morphology, plays a critical role in energy consumption estimation, urban microclimate modeling, 3D reconstruction, population distribution analysis, and urban planning [214]. Traditional methods, such as field surveys, are accurate but time-consuming and labor-intensive, making them unsuitable for large-scale applications. Remote sensing provides a cost-effective alternative but faces challenges: airborne LiDAR

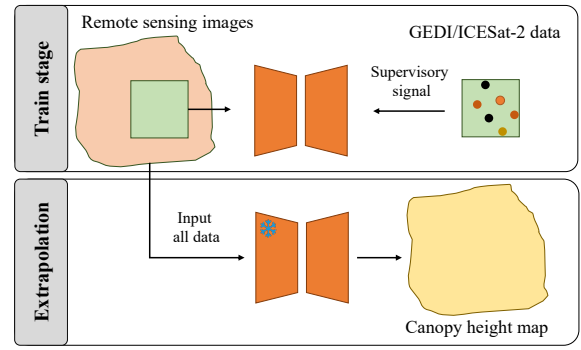


Figure 12: Canopy height map generation based on remote sensing images and GEDI/ICESat-2 data. In the training phase, remote sensing images and corresponding GEDI/ICESat-2 data are used to train the neural network. In the extrapolation phase, the complete remote sensing data is input into the model to generate the full canopy height map.

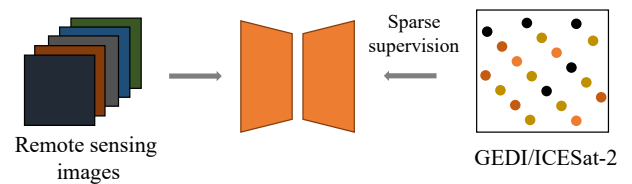


Figure 13: Illustration of the model training process with sparse supervision from GEDI/ICESat-2 LiDAR.

data are expensive, SAR data struggle with single-building delineation, and shadow-based methods using high-resolution optical imagery, though practical, often rely on image metadata and building height annotations while ignoring azimuth variations, limiting their applicability. ICESat-2 satellite ATL03 photon data offer high-precision building height measurements but are restricted by orbital coverage, allowing measurement of only a limited number of buildings, as shown in Fig. 14.

Current methods integrate ICESat-2 photon data with remote sensing imagery to leverage their combined strengths, overcoming limitations of traditional methods and improving accuracy and applicability in building height extraction. [215, 216, 217, 218, 219] train the model with small-scale data and generalize it to large-scale areas. For instance, Ma et al. [216] combine GEDI LiDAR data with features from Landsat-8, Sentinel-2, Sentinel-1, and terrain data to train random forest models across 68 subregions globally, generating a 150-meter resolution global urban building height map. Ma et al. [217] combine GEDI LiDAR, optical (Landsat-8, Sentinel-2), and radar (Sentinel-1) data to produce a 150-meter resolution

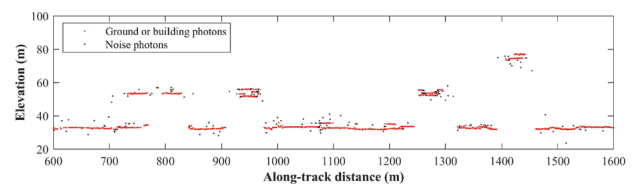


Figure 14: The result of candidate ground or building photons extraction. The image is obtained from [213].

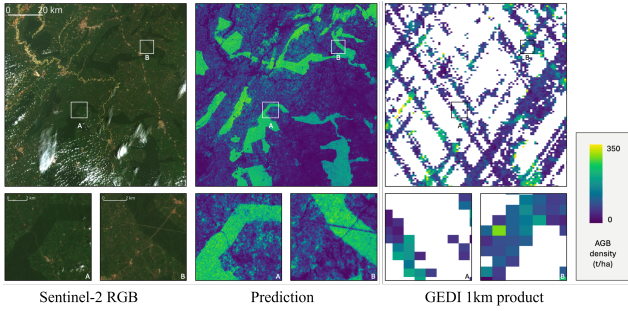


Figure 15: A high-resolution (10 m) map of AGB predictions. The image is obtained from [220].

building height map for the Yangtze River Delta using a random forest model to scale discrete GEDI samples to regional mapping. Kamath et al. [218] integrate LiDAR, ICESat-2, GEDI, and ALOS DSM data with machine learning to generate global building heights and urban canopy parameters (UCPs). Using LiDAR-derived nDSM and features like building area and population density, they train a Random Forest model to predict building heights, which is then applied to cities worldwide for urban climate simulations, thermal comfort assessments, and energy consumption predictions.

3.3. Biomass estimation

Aboveground biomass (AGB) plays a crucial role in global climate change, particularly in carbon absorption and carbon sequestration [220]. Accurate estimation of AGB is essential for sustainable forest management and biodiversity conservation, as shown in Fig. 15. However, existing estimation methods, such as traditional destructive sampling and remote sensing, face challenges related to accuracy, coverage, and data scarcity. Spaceborne lidar provides high-precision biomass data, but its coverage is limited. By integrating multi-source Earth observation data and advanced machine learning methods, these challenges can be addressed to generate high-quality biomass maps.

Current research [221, 222, 223, 224, 225, 226, 227, 228, 229, 230] often utilizes regression models, machine learning, or deep learning techniques combined with remote sensing imagery, airborne LiDAR, or satellite LiDAR data to train on small regions and then generalize to larger areas. Campbell et al. [221] combine ground measurements with airborne lidar (ALS) data to construct a local-scale random forest model for predicting aboveground biomass (AGB) within the ALS coverage. They then use the predictions of the local model as reference data and combine them with Landsat optical remote sensing data and GEDI lidar data to build a regional-scale model, enabling AGB estimation over a larger area. Jiang et al. [223] combine ICESat-2 lidar data and Sentinel-2 optical remote sensing data and use an optimized Extreme Learning Machine (ELM) algorithm to estimate the aboveground biomass (AGB) of natural forests in the eastern Tibetan Plateau. Vázquez-Alonso et al. [224] combine ground surveys, LiDAR data, and Sentinel-2 imagery with a random forest model to classify forest types and estimate aboveground biomass (AGB).

Using LiDAR-derived features, they build regression models to generate a high-resolution AGB map for a 25 km² area. Duncanson et al. [225] use ground and airborne lidar data from 74 global forest sites to generate training data with simulated GEDI waveforms. They develop stratified regression models based on relative height (RH) metrics, optimized by geographic and plant functional type (PFT) stratification, variable selection, and data transformation. Deng et al. [226] use ICESat-2 ATL08 LiDAR and multi-source remote sensing data (Landsat 8, Sentinel-1/2, DEM) with a random forest model to map 30-meter resolution canopy height. They further estimate forest aboveground biomass and carbon storage in Shangri-La City using height-DBH models and biomass formulas. Oehmck et al. [229] use deep learning models like PointNet, KPConv, and Minkowski CNNs to estimate above-ground biomass (AGB) and wood volume directly from airborne LiDAR point clouds. Leveraging 3D structural data, this method outperforms traditional statistical models and is applied to nationwide data in Denmark to create high-resolution biomass maps.

Additionally, a small number of studies use satellite LiDAR point clouds as **weak supervision signals**, combined with deep learning techniques, to map terrestrial biomass. Weber et al. [210] develop a deep learning model to predict global aboveground biomass density (AGBD), canopy height (CH), and canopy cover (CC) using 13-channel inputs from Sentinel-1/2, multispectral data, and DEMs. With GEDI LiDAR data as labels, the model employs a multi-head CNN architecture to simultaneously predict these variables and their uncertainties, enabling high-resolution global forest monitoring. Muszynski et al. [231] pre-train a Geospatial Foundation Model (GFM) with self-supervised learning, then fine-tune it on sparsely labeled data to estimate aboveground biomass (AGB) in Brazil. Using a Swin-B Transformer as the encoder, the model combines labeled and unlabeled data to improve generalization, achieving AGB estimation accuracy comparable to U-Net while reducing computational costs.

3.4. Summary and discussion

In remote sensing inversion tasks, traditional methods typically train models on small regions and apply them to the entire dataset. However, this approach often leads to significant errors when dealing with unseen data, affecting inversion accuracy. Using LiDAR data as weak supervision in combination with deep learning techniques and training jointly on large-scale datasets allows the model to learn broader features and shows great potential. However, existing research mainly focuses on network structure adjustments or pseudo-labeling, without fully leveraging weakly supervised learning techniques. Approaches such as contrastive learning, self-training, consistency loss, and active learning remain underexplored.

Moreover, remote sensing data are influenced by factors like geographic location, weather, seasonal variations, and sensor types, leading to significant domain shifts. Current research often assumes that data from different regions and times belong to the same domain, without fully utilizing domain adaptation techniques to address domain shift issues.

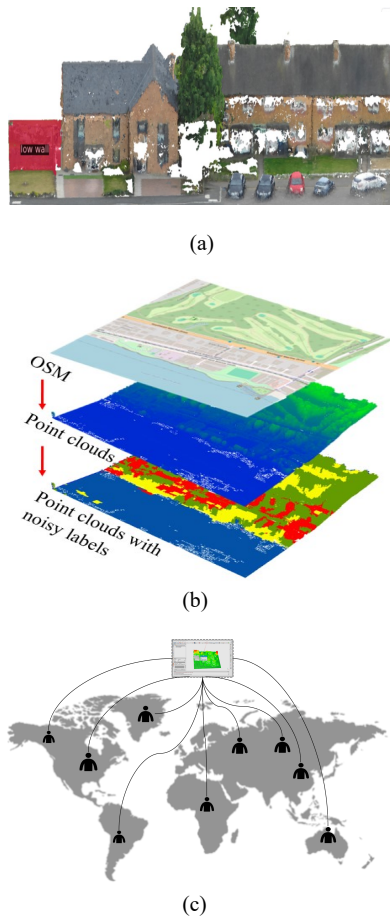


Figure 16: Different annotation methods. (a) based on foundation models [232], (b) based on historical maps, and (c) based on crowd-sourced data.

In conclusion, current remote sensing inversion methods largely rely on traditional statistical approaches, with relatively limited use of modern machine learning techniques, particularly weakly supervised learning, which can learn from imperfect data. Integrating weakly supervised learning into remote sensing inversion tasks can improve model accuracy and generalization and effectively address the complexities of remote sensing data, advancing inversion technologies.

4. Perspectives and Future Work

We have identified several promising research directions in the domain of weak supervision for LiDAR remote sensing:

Leveraging Ubiquitous Annotations. The development of large-scale models, including generative models and vision-language foundation models, has enabled the generation of vast quantities of annotations [134]. These models have already demonstrated significant success in annotating remote sensing imagery. Beyond these automated approaches, numerous sources of annotations are readily available, including crowd-sourced data [233], network-generated labels [234], historical maps (e.g., OpenStreetMap [235]), and annotations derived

from remote sensing images, as shown in Fig. 16. This abundance of annotation sources represents a valuable opportunity for advancing weakly supervised LiDAR interpretation. Future research should focus on fully harnessing these ubiquitous annotations to enhance the precision and efficiency of weakly supervised LiDAR-remote sensing tasks. By integrating these diverse annotation sources, researchers can reduce reliance on labor-intensive manual labeling, improve model performance, and significantly lower operational costs. The challenge lies in developing robust frameworks that can effectively utilize such diverse and sometimes noisy annotations to achieve consistent and scalable outcomes.

Domain Variability in LiDAR Remote Sensing. The dynamic nature of these phenomena—driven by temporal, seasonal, and regional variability—exacerbates the challenges of domain shifts [16]. These challenges are further amplified by the inherent modality inconsistencies among LiDAR systems, such as airborne (ALS), terrestrial (TLS), and spaceborne sensors, which differ in resolution, coverage, and acquisition geometry. The combination of domain variability and multimodal inconsistencies makes obtaining comprehensive, consistent annotations both expensive and infeasible, particularly given the high cost and complexity of point cloud labeling.

Weakly supervised learning offers a practical solution by leveraging limited labeled data and vast unlabeled datasets to mitigate annotation scarcity. Techniques such as semi-supervised learning [30, 31], feature alignment [23], and pseudo-labeling [32] are particularly suited to LiDAR data, utilizing its geometric and spatial properties. When combined with domain adaptation, these methods can address not only temporal and spatial domain shifts but also the modality gaps inherent to LiDAR systems.

Future LiDAR research must prioritize annotation-efficient and modality-robust approaches to handle domain and sensor variability. Weak supervision has the potential to enhance model generalization and adaptability, enabling LiDAR to address dynamic Earth observation challenges such as disaster response, urban monitoring, and environmental change analysis. By bridging technical gaps, weakly supervised learning can ensure LiDAR’s broader applicability in real-world, rapidly evolving scenarios.

LiDAR Remote Sensing Meets Open World. Current LiDAR remote sensing technologies have made significant progress in LiDAR interpretation and inversion. However, most existing methods focus on closed-set tasks, where neural networks are trained on a specific dataset and tested on the same category set. While effective for recognizing known classes, this approach struggles with the dynamic and uncertain nature of the real world, including unseen categories, environmental changes, and new tasks [236]. As a result, traditional closed-set methods are limited in addressing the diversity and complexity of the open world. Existing LiDAR datasets are relatively small and fixed in terms of categories. Future research should focus on developing LiDAR datasets with richer, more diverse categories that better reflect real-world scenarios. Additionally, integrating foundational models and multimodal data to develop cross-modal, generalizable, and scalable models will be a key

direction for future work.

New Paradigms for LiDAR Remote Sensing Retrieval. Most current approaches in LiDAR remote sensing involve extracting sparse signal-derived features, such as elevation or vegetation metrics, and using them to construct regression or classification models for large-scale remote sensing retrieval tasks. However, with the advancement of deep learning, there is growing interest in leveraging weak supervision to fuse LiDAR data with optical remote sensing imagery for improved retrieval accuracy [14]. Constructing spatiotemporally continuous remote sensing retrieval products using sparse supervision signals (e.g., LiDAR) [237]. This emerging paradigm raises two critical challenges: 1) how to effectively integrate multi-modal remote sensing data for retrieval tasks, and 2) how to utilize sparse LiDAR data as a weak supervisory signal to train deep learning models for large-scale retrieval.

Meanwhile, the use of LiDAR as a weak supervisory signal introduces unique challenges in training deep learning models. Sparse LiDAR data, despite its limitations, provides valuable ground truth for guiding retrieval tasks across large scales. Research efforts should focus on designing frameworks that can generalize from sparse supervisory signals, incorporating techniques like semi-supervised learning, transfer learning, and domain adaptation. These methods have the potential to unlock new applications in areas such as vegetation biomass estimation, urban morphology reconstruction, and hydrological modeling.

Datasets for LiDAR Remote Sensing. For large-scale environmental and geophysical parameter inversion, such as biomass estimation, LiDAR can serve as a critical weak supervision signal [210, 231]. However, the lack of comprehensive, large-scale LiDAR datasets tailored to these tasks limits its potential. High-resolution LiDAR data integrated with other remote sensing modalities could bridge this gap, enabling more accurate and scalable models for remote sensing applications [238].

In the domain generalization context, the absence of datasets facilitating cross-modal, cross-season and cross-platform transfer learning poses significant challenges. Current datasets are predominantly developed for autonomous driving and lack the scope and diversity required for Earth observation. For example, cross-modal datasets enabling the transfer of knowledge between space-borne, airborne (ALS), and terrestrial (TLS) LiDAR remain unavailable. Such datasets are essential for studying domain gaps and advancing domain adaptation techniques for varying acquisition geometries and resolutions—key challenges in remote sensing.

Moreover, the scarcity of multimodal datasets combining LiDAR with optical, radar, or hyperspectral remote sensing data further constrains progress. Cross-modality datasets with aligned labels are critical for fostering weakly supervised learning and enabling models to leverage complementary information across sensing modalities.

Future efforts should prioritize building large-scale, multimodal, and cross-platform LiDAR datasets for remote sensing. These datasets will form the foundation for developing weak supervision techniques and addressing core challenges in do-

main generalization, ultimately advancing the applicability of LiDAR in dynamic and large-scale Earth observation tasks.

LiDAR Remote Sensing Meets LM. The integration of LiDAR remote sensing with large-scale models offers significant potential for Earth observation. LiDAR provides high-resolution 3D spatial data, and when combined with pre-trained models for remote sensing images, it enables robust and scalable solutions for tasks such as biomass estimation and terrain analysis. Furthermore, integrating LiDAR data with multi-modal large models (e.g., vision-language models) can address challenges such as parameter inversion and scene interpretation [239]. Cross-modal supervision allows the model to leverage text, imagery, and other information to provide supervisory signals for LiDAR tasks, enabling weak supervision at scale. For a given 3D pre-trained large-scale model in the future, it could be applied to Earth observation. Pre-training on diverse 3D Earth observations can significantly improve the model’s ability to address the inherent complexities and domain shift in remote sensing.

5. Conclusion

In summary, we present the first comprehensive overview of LiDAR remote sensing from a machine learning perspective. For LiDAR interpretation, we discuss key tasks such as semantic segmentation, instance segmentation, and object detection, emphasizing the latest methods and related weakly supervised learning techniques. In the context of LiDAR inversion, we focus on applications like canopy height estimation, building height estimation, and biomass inversion. Although weak supervision is increasingly being applied to inversion tasks, existing methods are still limited and have yet to fully harness the potential of weakly supervised learning.

We also propose several promising research directions for further exploration, including better utilization of widely available annotations, applying weak supervision to address domain shift in LiDAR remote sensing, developing new paradigms for LiDAR inversion, proposing new inversion datasets, and exploring large model development and generalized models for open-world environments. Through these explorations, the gap between point cloud interpretation and remote sensing applications could be bridged using machine learning (e.g., weakly supervised learning), advancing LiDAR remote sensing.

Acknowledgements

This work was supported by the National Natural Science Foundation of China under Grant 42201481 and the National Key R&D Program of China (2024YFF0810400).

References

- [1] Y. Chen, S. Zhang, T. Han, Y. Du, W. Zhang, J. Li, Chat3d: Interactive understanding 3d scene-level point clouds by chatting with foundation model for urban ecological construction, *ISPRS Journal of Photogrammetry and Remote Sensing* 212 (2024) 181–192.

- [2] C. Wang, X. Yang, X. Xi, S. Nie, P. Dong, Introduction to lidar remote sensing, 2024.
- [3] X. Zhu, S. Nie, C. Wang, X. Xi, J. Wang, D. Li, H. Zhou, A noise removal algorithm based on optics for photon-counting lidar data, *IEEE Geoscience and Remote Sensing Letters* 18 (2020) 1471–1475.
- [4] J. Duan, H. Wang, C. Wang, S. Nie, X. Yang, X. Xi, Denoising and classification of urban icesat-2 photon data fused with sentinel-2 spectral images, *International Journal of Digital Earth* 16 (2023) 4346–4367.
- [5] X. Yang, C. Wang, X. Xi, Z. Niu, D. Li, S. Nie, K. Bi, R. Wang, Assessment of multiple scattering in lidar canopy waveform, *IEEE Journal of Selected Topics in Applied Earth Observations and Remote Sensing* 17 (2024) 14394–14407.
- [6] X. Wu, X. Xi, C. Luo, C. Wang, S. Nie, Line segment descriptor-based efficient coarse registration for forest tls-uls point clouds, *IEEE Transactions on Geoscience and Remote Sensing* 62 (2024) 1–12.
- [7] N. Varney, V. K. Asari, Q. Graehling, Dales: A large-scale aerial lidar data set for semantic segmentation, in: 2020 IEEE/CVF Conference on Computer Vision and Pattern Recognition Workshops (CVPRW), 2020, pp. 717–726.
- [8] X. Han, C. Liu, Y. Zhou, K. Tan, Z. Dong, B. Yang, Whu-urban3d: An urban scene lidar point cloud dataset for semantic instance segmentation, *ISPRS Journal of Photogrammetry and Remote Sensing* 209 (2024) 500–513.
- [9] Y. Qiao, X. Xi, C. Wang, M. Du, S. Nie, W. Liu, H. Fan, A framework for automated reconstruction of communication towers from terrestrial laser scanning point clouds, *International Journal of Digital Earth* 17 (2024) 2366431.
- [10] Z. Qin, H. Yang, Q. Shu, J. Yu, L. Xu, M. Wang, C. Xia, D. Duan, Estimation of leaf area index for dendrocalamus giganteus based on multi-source remote sensing data, *Forests* 15 (2024).
- [11] S. Kacimi, R. Kwok, Two decades of arctic sea-ice thickness from satellite altimeters: Retrieval approaches and record of changes (2003–2023), *Remote Sensing* 16 (2024).
- [12] H. Besso, D. Shean, J. D. Lundquist, Mountain snow depth retrievals from customized processing of icesat-2 satellite laser altimetry, *Remote Sensing of Environment* 300 (2024) 113843.
- [13] S. Xia, J. Yue, K. Kania, L. Fang, A. Tagliasacchi, K. M. Yi, W. Sun, Densify your labels: Unsupervised clustering with bipartite matching for weakly supervised point cloud segmentation, 2023. [arXiv:2312.06799](https://arxiv.org/abs/2312.06799).
- [14] N. Lang, W. Jetz, K. Schindler, J. D. Wegner, A high-resolution canopy height model of the earth, *Nature Ecology & Evolution* 7 (2023) 1778–1789.
- [15] J. Tolan, H.-I. Yang, B. Nosarzewski, G. Couairon, H. V. Vo, J. Brandt, J. Spore, S. Majumdar, D. Haziza, J. Vamaraju, T. Moutakanni, P. Bojanowski, T. Johns, B. White, T. Tiecke, C. Couprie, Very high resolution canopy height maps from rgb imagery using self-supervised vision transformer and convolutional decoder trained on aerial lidar, *Remote Sensing of Environment* 300 (2024) 113888.
- [16] P. Wang, W. Yao, J. Shao, Z. He, Test-time adaptation for geospatial point cloud semantic segmentation with distinct domain shifts, [ArXiv abs/2407.06043](https://arxiv.org/abs/2407.06043) (2024).
- [17] M. Brandt, J. Chave, S. Li, R. Fensholt, P. Ciais, J.-P. Wigneron, F. Gieseke, S. Saatchi, C. Tucker, C. Igel, High-resolution sensors and deep learning models for tree resource monitoring, *Nature Reviews Electrical Engineering* (2024) 1–14.
- [18] P. Wang, W. Yao, A new weakly supervised approach for als point cloud semantic segmentation, *ISPRS Journal of Photogrammetry and Remote Sensing* 188 (2022) 237–254.
- [19] X. Xu, G. H. Lee, Weakly Supervised Semantic Point Cloud Segmentation: Towards 10× Fewer Labels, in: 2020 IEEE/CVF Conference on Computer Vision and Pattern Recognition (CVPR), IEEE, Seattle, WA, USA, 2020, pp. 13703–13712.
- [20] H. Li, Z. Sun, Y. Wu, Y. Song, Semi-supervised point cloud segmentation using self-training with label confidence prediction, *Neurocomputing* 437 (2021) 227–237.
- [21] K. Sohn, Z. Zhang, C.-L. Li, H. Zhang, C.-Y. Lee, T. Pfister, A simple semi-supervised learning framework for object detection, 2020. [arXiv:2005.04757](https://arxiv.org/abs/2005.04757).
- [22] Z. Xu, B. Yuan, S. Zhao, Q. Zhang, X. Gao, Hierarchical Point-based Active Learning for Semi-supervised Point Cloud Semantic Segmentation, in: 2023 IEEE/CVF International Conference on Computer Vision (ICCV), IEEE, Paris, France, 2023, pp. 18052–18062.
- [23] H. Luo, K. Khoshelham, L. Fang, C. Chen, Unsupervised scene adaptation for semantic segmentation of urban mobile laser scanning point clouds, *Isprs Journal of Photogrammetry and Remote Sensing* 169 (2020) 253–267.
- [24] M. Kölle, D. Laupheimer, S. Schmohl, N. Haala, F. Rottensteiner, J. D. Wegner, H. Ledoux, The hessigheim 3d (h3d) benchmark on semantic segmentation of high-resolution 3d point clouds and textured meshes from uav lidar and multi-view-stereo, *ISPRS Open Journal of Photogrammetry and Remote Sensing* 1 (2021) 100001.
- [25] E. Guenther, L. Magruder, A. Neuenschwander, D. Maze-England, J. Dietrich, Examining cnn terrain model for tandem-x dems using icesat-2 data in southeastern united states, *Remote Sensing of Environment* 311 (2024) 114293.
- [26] A. Xiao, X. Zhang, L. Shao, S. Lu, A survey of label-efficient deep learning for 3d point clouds, *IEEE Transactions on Pattern Analysis and Machine Intelligence* 46 (2024) 9139–9160.
- [27] Y. Guo, H. Wang, Q. Hu, H. Liu, L. Liu, M. Bennamoun, Deep learning for 3d point clouds: A survey, *IEEE Transactions on Pattern Analysis and Machine Intelligence* 43 (2021) 4338–4364.
- [28] Y. He, H. Yu, X. Liu, Z. Yang, W. Sun, S. Anwar, A. Mian, Deep learning based 3d segmentation in computer vision: A survey, *Information Fusion* 115 (2025) 102722.
- [29] A. Xiao, J. Huang, D. Guan, X. Zhang, S. Lu, L. Shao, Unsupervised point cloud representation learning with deep neural networks: A survey, *IEEE Transactions on Pattern Analysis and Machine Intelligence* 45 (2023) 11321–11339.
- [30] W. Liao, J. Xia, P. Du, W. Philips, Semi-supervised graph fusion of hyperspectral and lidar data for classification, in: 2015 IEEE International Geoscience and Remote Sensing Symposium (IGARSS), 2015, pp. 53–56.
- [31] Z. Li, Y. Wang, L. Wang, F. Guo, Y. Yang, J. Wei, Pseudolabeling contrastive learning for semisupervised hyperspectral and lidar data classification, *IEEE Journal of Selected Topics in Applied Earth Observations and Remote Sensing* 17 (2024) 17099–17116.
- [32] J. Li, Y. Ma, R. Song, B. Xi, D. Hong, Q. Du, A triplet semisupervised deep network for fusion classification of hyperspectral and lidar data, *IEEE Transactions on Geoscience and Remote Sensing* 60 (2022) 1–13.
- [33] F. Guo, Z. Li, Q. Meng, G. Ren, L. Wang, J. Wang, H. Qin, J. Zhang, Semi-supervised cross-domain feature fusion classification network for coastal wetland classification with hyperspectral and lidar data, *Int. J. Appl. Earth Obs. Geoinformation* 120 (2023) 103354.
- [34] C. Pu, Y. Liu, S. Lin, X. Shi, Z. Li, H. Huang, Multimodal deep learning for semisupervised classification of hyperspectral and lidar data, *IEEE Transactions on Big Data* (2024) 1–14.
- [35] S. Dersch, A. Schöttl, P. Krzystek, M. Heurich, Semi-supervised multi-class tree crown delineation using aerial multispectral imagery and lidar data, *ISPRS Journal of Photogrammetry and Remote Sensing* (2024).
- [36] P. Wang, W. Yao, Weakly Supervised Pseudo-Label assisted Learning for ALS Point Cloud Semantic Segmentation, 2021. [ArXiv:2105.01919 \[cs\]](https://arxiv.org/abs/2105.01919).
- [37] X. Lei, H. Guan, L. Ma, Y. Yu, Z. Dong, K. Gao, M. Reza Delavar, J. Li, WSPointNet: A multi-branch weakly supervised learning network for semantic segmentation of large-scale mobile laser scanning point clouds, *International Journal of Applied Earth Observation and Geoinformation* 115 (2022) 103129.
- [38] X. Lei, H. Guan, L. Ma, J. Liu, Y. Yu, L. Wang, Z. Dong, H. Ni, J. Li, Daal-ws: A weakly-supervised method integrated with data augmentation and active learning strategies for mls point cloud semantic segmentation, *International Journal of Applied Earth Observation and Geoinformation* 131 (2024) 103970.
- [39] Y. Lin, G. Vosselman, M. Y. Yang, Weakly supervised semantic segmentation of airborne laser scanning point clouds, *ISPRS Journal of Photogrammetry and Remote Sensing* 187 (2022) 79–100.
- [40] P. Wang, W. Yao, J. Shao, One class one click: Quasi scene-level weakly supervised point cloud semantic segmentation with active learning, *ISPRS Journal of Photogrammetry and Remote Sensing* 204 (2023) 89–104.
- [41] Y. Gao, S. Xia, C. Wang, X. Xi, B. Yang, C. Xie, Semantic segmentation of airborne lidar point clouds with noisy labels, *IEEE Transactions on*

- Geoscience and Remote Sensing 62 (2024) 1–14.
- [42] S. Peng, X. Xi, C. Wang, R. Xie, P. Wang, H. Tan, Point-based multilevel domain adaptation for point cloud segmentation, *IEEE Geoscience and Remote Sensing Letters* 19 (2020) 1–5.
- [43] Y. Xie, K. Schindler, J. Tian, X. X. Zhu, Exploring cross-city semantic segmentation of als point clouds, *The International Archives of the Photogrammetry, Remote Sensing and Spatial Information Sciences* (2021).
- [44] S. Shen, Y. Xia, A. Eich, Y. Xu, B. Yang, U. Stilla, Segtrans: Semantic segmentation with transfer learning for mls point clouds, *IEEE Geoscience and Remote Sensing Letters* 20 (2023) 1–5.
- [45] M. Wang, X. Qiu, Z. Zhang, S. Gao, A domain adaptation framework for cross-modality sar 3d reconstruction point clouds segmentation utilizing lidar data, *Int. J. Appl. Earth Obs. Geoinformation* 133 (2024) 104103.
- [46] Q. Wang, M. Wang, J. Huang, T. Liu, T. Shen, Y. Gu, Unsupervised domain adaptation for cross-scene multispectral point cloud classification, *IEEE Transactions on Geoscience and Remote Sensing* 62 (2024) 1–15.
- [47] Z.-H. Zhou, A brief introduction to weakly supervised learning, *National Science Review* 5 (2018) 44–53.
- [48] W. M. Kouw, M. Loog, A review of domain adaptation without target labels, *IEEE Transactions on Pattern Analysis and Machine Intelligence* 43 (2021) 766–785.
- [49] J. Yue, L. Fang, P. Ghamisi, W. Xie, J. Li, J. Chanussot, A. Plaza, Optical remote sensing image understanding with weak supervision: Concepts, methods, and perspectives, *IEEE Geoscience and Remote Sensing Magazine* 10 (2022) 250–269.
- [50] A. Xiao, X. Zhang, L. Shao, S. Lu, A survey of label-efficient deep learning for 3d point clouds, 2023. [arXiv:2305.19812](https://arxiv.org/abs/2305.19812).
- [51] W. Shen, Z. Peng, X. Wang, H. Wang, J. Cen, D. Jiang, L. Xie, X. Yang, Q. Tian, A survey on label-efficient deep image segmentation: Bridging the gap between weak supervision and dense prediction, *IEEE Transactions on Pattern Analysis and Machine Intelligence* 45 (2023) 9284–9305.
- [52] Z. Liu, X. Qi, C.-W. Fu, One thing one click: A self-training approach for weakly supervised 3d semantic segmentation, 2021. [arXiv:2104.02246](https://arxiv.org/abs/2104.02246).
- [53] Y. Zhang, Z. Li, Y. Xie, Y. Qu, C. Li, T. Mei, Weakly supervised semantic segmentation for large-scale point cloud, *ArXiv abs/2212.04744* (2021).
- [54] C. Liu, C. Gao, F. Liu, J. Liu, D. Meng, X. Gao, Ss3d: Sparsely-supervised 3d object detection from point cloud, in: 2022 IEEE/CVF Conference on Computer Vision and Pattern Recognition (CVPR), 2022, pp. 8418–8427.
- [55] Q. Hu, B. Yang, G. Fang, Y. Guo, A. Leonardis, N. Trigoni, A. Markham, Sqn: Weakly-supervised semantic segmentation of large-scale 3d point clouds, 2023. [arXiv:2104.04891](https://arxiv.org/abs/2104.04891).
- [56] L. Jiang, S. Shi, Z. Tian, X. Lai, S. Liu, C.-W. Fu, J. Jia, Guided Point Contrastive Learning for Semi-supervised Point Cloud Semantic Segmentation, in: 2021 IEEE/CVF International Conference on Computer Vision (ICCV), IEEE, Montreal, QC, Canada, 2021, pp. 6403–6412.
- [57] Y. Zhang, Y. Liao, C. Ye, Semi-supervised point cloud semantic segmentation with mean teacher, in: 2021 2nd International Seminar on Artificial Intelligence, Networking and Information Technology (AINIT), 2021, pp. 479–483.
- [58] S. Deng, Q. Dong, B. Liu, Z. Hu, Superpoint-guided Semi-supervised Semantic Segmentation of 3D Point Clouds, 2021. [ArXiv:2107.03601](https://arxiv.org/abs/2107.03601) [cs].
- [59] M. Cheng, L. Hui, J. Xie, J. Yang, Spsc-net: Semi-supervised semantic 3d point cloud segmentation network, 2021. [arXiv:2104.07861](https://arxiv.org/abs/2104.07861).
- [60] L. Kong, J. Ren, L. Pan, Z. Liu, LaserMix for Semi-Supervised LiDAR Semantic Segmentation, in: 2023 IEEE/CVF Conference on Computer Vision and Pattern Recognition (CVPR), IEEE, Vancouver, BC, Canada, 2023, pp. 21706–21716.
- [61] L. Li, H. P. H. Shum, T. Breckon, Less is more: Reducing task and model complexity for 3d point cloud semantic segmentation, *ArXiv abs/2303.11203* (2023).
- [62] Y. Liu, Y. Chen, H. Wang, V. Belagiannis, I. Reid, G. Carneiro, Ittakestwo: Leveraging peer representations for semi-supervised lidar semantic segmentation, *ArXiv abs/2407.07171* (2024).
- [63] J. Jeong, S. Lee, J. Kim, N. Kwak, Consistency-based semi-supervised learning for object detection, in: H. Wallach, H. Larochelle, A. Beygelzimer, F. d'Alché-Buc, E. Fox, R. Garnett (Eds.), *Advances in Neural Information Processing Systems*, volume 32, Curran Associates, Inc., 2019.
- [64] N. Zhao, T.-S. Chua, G. H. Lee, Sess: Self-ensembling semi-supervised 3d object detection, 2021. [arXiv:1912.11803](https://arxiv.org/abs/1912.11803).
- [65] H. Wang, Y. Cong, O. Litany, Y. Gao, L. J. Guibas, 3dioumatch: Leveraging iou prediction for semi-supervised 3d object detection, in: 2021 IEEE/CVF Conference on Computer Vision and Pattern Recognition (CVPR), 2021, pp. 14610–14619.
- [66] X. Zhu, H. Zhou, T. Wang, F. Hong, W. Li, Y. Ma, H. Li, R. Yang, D. Lin, Cylindrical and asymmetrical 3d convolution networks for lidar-based perception, *IEEE Transactions on Pattern Analysis and Machine Intelligence* 44 (2022) 6807–6822.
- [67] C. R. Qi, Y. Zhou, M. Najibi, P. Sun, K. Vo, B. Deng, D. Anguelov, Offboard 3d object detection from point cloud sequences, in: 2021 IEEE/CVF Conference on Computer Vision and Pattern Recognition (CVPR), 2021, pp. 6130–6140.
- [68] H. Xu, F. Liu, Q. Zhou, J. Hao, Z. Cao, Z. Feng, L. Ma, Semi-supervised 3d object detection via adaptive pseudo-labeling, in: 2021 IEEE International Conference on Image Processing (ICIP), 2021, pp. 3183–3187.
- [69] J. Wang, H. Gang, S. Ancha, Y.-T. Chen, D. Held, Semi-supervised 3d object detection via temporal graph neural networks, in: 2021 International Conference on 3D Vision (3DV), 2021, pp. 413–422.
- [70] J. Yin, J. Fang, D. Zhou, L. Zhang, C.-Z. Xu, J. Shen, W. Wang, Semi-supervised 3d object detection with proficient teachers, in: *European Conference on Computer Vision*, Springer, 2022, pp. 727–743.
- [71] C. Liu, C. Gao, F. Liu, P. Li, D. Meng, X. Gao, Hierarchical supervision and shuffle data augmentation for 3d semi-supervised object detection, in: 2023 IEEE/CVF Conference on Computer Vision and Pattern Recognition (CVPR), 2023, pp. 23819–23828.
- [72] X. Wu, L. Peng, L. Xie, Y. Hou, B. Lin, X. Huang, H. Liu, D. Cai, W. Ouyang, Semi-supervised 3d object detection with patchteacher and pillarmix, in: *AAAI Conference on Artificial Intelligence*, 2024.
- [73] S. Wong, Ssf3d: Strict semi-supervised 3d object detection with switching filter, 2024. [arXiv:2403.17390](https://arxiv.org/abs/2403.17390).
- [74] Y. Liao, H. Zhu, T. Chen, J. Fan, Spcr: semi-supervised point cloud instance segmentation with perturbation consistency regularization, in: 2021 IEEE International Conference on Image Processing (ICIP), 2021, pp. 3113–3117.
- [75] Y. Liao, H. Zhu, Y. ting Zhang, C. Ye, T. Chen, J. Fan, Point cloud instance segmentation with semi-supervised bounding-box mining, *IEEE Transactions on Pattern Analysis and Machine Intelligence* 44 (2021) 10159–10170.
- [76] R. Chu, X. Ye, Z. Liu, X. Tan, X. Qi, C.-W. Fu, J. Jia, Twist: Two-way inter-label self-training for semi-supervised 3d instance segmentation, in: 2022 IEEE/CVF Conference on Computer Vision and Pattern Recognition (CVPR), 2022, pp. 1090–1099.
- [77] K. Liu, Y. Zhao, Q. Nie, Z. Gao, B. M. Chen, Weakly supervised 3d scene segmentation with region-level boundary awareness and instance discrimination, in: *European conference on computer vision*, Springer, 2022, pp. 37–55.
- [78] Y. Zhang, Y. Qu, Y. Xie, Z. Li, S. Zheng, C. Li, Perturbed Self-Distillation: Weakly Supervised Large-Scale Point Cloud Semantic Segmentation, in: 2021 IEEE/CVF International Conference on Computer Vision (ICCV), IEEE, Montreal, QC, Canada, 2021, pp. 15500–15508.
- [79] M. Li, Y. Xie, Y. Shen, B. Ke, R. Qiao, B. Ren, S. Lin, L. Ma, HybridCR: Weakly-Supervised 3D Point Cloud Semantic Segmentation via Hybrid Contrastive Regularization, in: 2022 IEEE/CVF Conference on Computer Vision and Pattern Recognition (CVPR), IEEE, New Orleans, LA, USA, 2022, pp. 14910–14919.
- [80] Z. Hu, X. Bai, R. Zhang, X. Wang, G. Sun, H. Fu, C.-L. Tai, LiDAL: Inter-frame Uncertainty Based Active Learning for 3D LiDAR Semantic Segmentation, 2022. [ArXiv:2211.05997](https://arxiv.org/abs/2211.05997) [cs].
- [81] J. Zhao, W. Huang, H. Wu, C. Wen, B. Yang, Y. Guo, C. Wang, SemanticFlow: Semantic Segmentation of Sequential LiDAR Point Clouds From Sparse Frame Annotations, *IEEE Transactions on Geoscience and Remote Sensing* 61 (2023) 1–11.
- [82] W. Huang, P. Zou, Y. Xia, C. Wen, Y. Zang, C. Wang, G. Zhou, OPOCA: One Point One Class Annotation for LiDAR Point Cloud Semantic Segmentation, *IEEE Transactions on Geoscience and Remote Sensing* 62 (2024) 1–10.
- [83] M. Li, Y. Xie, Y. Shen, B. Ke, R. Qiao, B. Ren, S. Lin, L. Ma, HybridCR:

- Weakly-Supervised 3D Point Cloud Semantic Segmentation via Hybrid Contrastive Regularization, in: 2022 IEEE/CVF Conference on Computer Vision and Pattern Recognition (CVPR), IEEE, New Orleans, LA, USA, 2022, pp. 14910–14919.
- [84] Q. Hu, B. Yang, G. Fang, Y. Guo, A. Leonardis, N. Trigoni, A. Markham, SQN: Weakly-Supervised Semantic Segmentation of Large-Scale 3D Point Clouds, 2023. [ArXiv:2104.04891 \[cs\]](#).
- [85] Z. Pan, N. Zhang, W. Gao, S. Liu, G. Li, Less Is More: Label Recommendation for Weakly Supervised Point Cloud Semantic Segmentation, Proceedings of the AAAI Conference on Artificial Intelligence 38 (2024) 4397–4405.
- [86] M. Liu, Y. Zhou, C. R. Qi, B. Gong, H. Su, D. Anguelov, LESS: Label-Efficient Semantic Segmentation for LiDAR Point Clouds, 2022. [ArXiv:2210.08064 \[cs\]](#).
- [87] T. Sun, Z. Zhang, X. Tan, Y. Qu, Y. Xie, Image understands point cloud: Weakly supervised 3d semantic segmentation via association learning, IEEE Transactions on Image Processing 33 (2024) 1838–1852.
- [88] Y. Chen, Z. Xu, Xiaoshui Huang, R. Zhang, X. Jiang, X. Gao, Weakly supervised lidar semantic segmentation via scatter image annotation, 2024. [arXiv:2404.12861](#).
- [89] X. Xu, Y. Wang, Y. Zheng, Y. Rao, J. Zhou, J. Lu, Back to reality: Weakly-supervised 3d object detection with shape-guided label enhancement, in: 2022 IEEE/CVF Conference on Computer Vision and Pattern Recognition (CVPR), 2022, pp. 8428–8437.
- [90] Q. Meng, W. Wang, T. Zhou, J. Shen, Y. Jia, L. Van Gool, Towards a weakly supervised framework for 3d point cloud object detection and annotation, IEEE Transactions on Pattern Analysis and Machine Intelligence 44 (2022) 4454–4468.
- [91] Q. Xia, J. Deng, C. Wen, H. Wu, S. Shi, X. Li, C. Wang, Coin: Contrastive instance feature mining for outdoor 3d object detection with very limited annotations, 2023 IEEE/CVF International Conference on Computer Vision (ICCV) (2023) 6231–6240.
- [92] D. Zhang, D. Liang, Z. Zou, J. Li, X. Ye, Z. Liu, X. Tan, X. Bai, A simple vision transformer for weakly semi-supervised 3d object detection, in: 2023 IEEE/CVF International Conference on Computer Vision (ICCV), 2023, pp. 8339–8349.
- [93] Y. Yang, L. Fan, Z. Zhang, Mixsup: Mixed-grained supervision for label-efficient lidar-based 3d object detection, [ArXiv abs/2401.16305 \(2024\)](#).
- [94] H. Gao, Z. Chen, Z. Chen, L. Chen, J. Liu, S. Zhang, F. Zhao, Leveraging imagery data with spatial point prior for weakly semi-supervised 3d object detection, [ArXiv abs/2403.15317 \(2024\)](#).
- [95] L. Chen, T. Yang, X. Zhang, W. Zhang, J. Sun, Points as queries: Weakly semi-supervised object detection by points, 2021. [arXiv:2104.07434](#).
- [96] J. Hou, B. Graham, M. Nießner, S. Xie, Exploring data-efficient 3d scene understanding with contrastive scene contexts, in: 2021 IEEE/CVF Conference on Computer Vision and Pattern Recognition (CVPR), 2021, pp. 15582–15592.
- [97] S. Xie, J. Gu, D. Guo, C. R. Qi, L. Guibas, O. Litany, Pointcontrast: Un-supervised pre-training for 3d point cloud understanding, in: Computer Vision—ECCV 2020: 16th European Conference, Glasgow, UK, August 23–28, 2020, Proceedings, Part III 16, Springer, 2020, pp. 574–591.
- [98] A. Tao, Y. Duan, Y. Wei, J. Lu, J. Zhou, Seggroup: Seg-level supervision for 3d instance and semantic segmentation, IEEE Transactions on Image Processing 31 (2022) 4952–4965.
- [99] L. Tang, L. Hui, J. Xie, Learning inter-superpoint affinity for weakly supervised 3d instance segmentation, in: Proceedings of the Asian Conference on Computer Vision, 2022, pp. 1282–1297.
- [100] L. Liu, T. Kong, M. Zhu, J. Fan, L. Fang, Clickseg: 3d instance segmentation with click-level weak annotations, [arXiv preprint arXiv:2307.09732 \(2023\)](#).
- [101] S. Dong, G. Lin, Weakly supervised 3d instance segmentation without instance-level annotations, [arXiv preprint arXiv:2308.01721 \(2023\)](#).
- [102] S. Dong, R. Li, J. Wei, F. Liu, G. Lin, Collaborative propagation on multiple instance graphs for 3d instance segmentation with single-point supervision, in: Proceedings of the IEEE/CVF International Conference on Computer Vision, 2023, pp. 16665–16674.
- [103] J. Wei, G. Lin, K.-H. Yap, T.-Y. Hung, L. Xie, Multi-Path Region Mining for Weakly Supervised 3D Semantic Segmentation on Point Clouds, in: 2020 IEEE/CVF Conference on Computer Vision and Pattern Recognition (CVPR), IEEE, Seattle, WA, USA, 2020, pp. 4383–4392.
- [104] Y. Liu, Q. Hu, Y. Lei, K. Xu, J. Li, Y. Guo, Box2Seg: Learning Semantics of 3D Point Clouds with Box-Level Supervision, 2022. [ArXiv:2201.02963 \[cs\]](#).
- [105] O. Unal, D. Dai, L. V. Gool, Scribble-supervised lidar semantic segmentation, 2022 IEEE/CVF Conference on Computer Vision and Pattern Recognition (CVPR) (2022) 2687–2697.
- [106] Y. Liao, H. Zhu, Y. Zhang, C. Ye, T. Chen, J. Fan, Point cloud instance segmentation with semi-supervised bounding-box mining, IEEE Transactions on Pattern Analysis and Machine Intelligence 44 (2021) 10159–10170.
- [107] T. D. Ngo, B.-S. Hua, K. Nguyen, Gapro: Box-supervised 3d point cloud instance segmentation using gaussian processes as pseudo labelers, in: Proceedings of the IEEE/CVF International Conference on Computer Vision, 2023, pp. 17794–17803.
- [108] H. Du, X. Yu, F. Hussain, M. A. Armin, L. Petersson, W. Li, Weakly-supervised point cloud instance segmentation with geometric priors, in: Proceedings of the IEEE/CVF Winter Conference on Applications of Computer Vision, 2023, pp. 4271–4280.
- [109] J. Chibane, F. Engelmann, T. Anh Tran, G. Pons-Moll, Box2mask: Weakly supervised 3d semantic instance segmentation using bounding boxes, in: European conference on computer vision, Springer, 2022, pp. 681–699.
- [110] Q. Yu, H. Du, X. Yu, A new perspective of weakly supervised 3d instance segmentation via bounding boxes, in: Australasian Joint Conference on Artificial Intelligence, Springer, 2023, pp. 103–114.
- [111] Q. Yu, H. Du, C. Liu, X. Yu, When 3d bounding-box meets sam: Point cloud instance segmentation with weak-and-noisy supervision, in: Proceedings of the IEEE/CVF Winter Conference on Applications of Computer Vision, 2024, pp. 3719–3728.
- [112] J. Lu, J. Deng, T. Zhang, Bsnnet: Box-supervised simulation-assisted mean teacher for 3d instance segmentation, in: Proceedings of the IEEE/CVF Conference on Computer Vision and Pattern Recognition, 2024, pp. 20374–20384.
- [113] Z. Ren, I. Misra, A. G. Schwing, R. Girdhar, 3d spatial recognition without spatially labeled 3d, 2021. [arXiv:2105.06461](#).
- [114] C.-K. Yang, J.-J. Wu, K.-S. Chen, Y.-Y. Chuang, Y.-Y. Lin, An mild-derived transformer for weakly supervised point cloud segmentation, in: Proceedings of the IEEE/CVF Conference on Computer Vision and Pattern Recognition (CVPR), 2022, pp. 11830–11839.
- [115] C.-K. Yang, M.-H. Chen, Y.-Y. Chuang, Y.-Y. Lin, 2d-3d interlaced transformer for point cloud segmentation with scene-level supervision, in: Proceedings of the IEEE/CVF International Conference on Computer Vision, 2023, pp. 977–987.
- [116] X. Li, Q. Xu, J. Zhang, T. Zhang, Q. Yu, L. Sheng, D. Xu, Multi-modality affinity inference for weakly supervised 3d semantic segmentation, 2023. [arXiv:2312.16578](#).
- [117] F. Rottensteiner, G. Sohn, J. Jung, M. Gerke, C. Baillard, S. Bénéitez, U. Breitkopf, The isprs benchmark on urban object classification and 3d building reconstruction, ISPRS Annals of the Photogrammetry, Remote Sensing and Spatial Information Sciences (2012) 293–298.
- [118] Q. Meng, W. Wang, T. Zhou, J. Shen, L. V. Gool, D. Dai, Weakly supervised 3d object detection from lidar point cloud, 2020. [arXiv:2007.11901](#).
- [119] Z. Qin, J. Wang, Y. Lu, Weakly supervised 3d object detection from point clouds, 2020. [arXiv:2007.13970](#).
- [120] Y. Wei, S. Su, J. Lu, J. Zhou, Fgr: Frustum-aware geometric reasoning for weakly supervised 3d vehicle detection, in: 2021 IEEE International Conference on Robotics and Automation (ICRA), 2021, pp. 4348–4354.
- [121] B. Han, Q. Yao, X. Yu, G. Niu, M. Xu, W. Hu, I. W.-H. Tsang, M. Sugiyama, Co-teaching: Robust training of deep neural networks with extremely noisy labels, in: Neural Information Processing Systems, 2018.
- [122] H. Song, M. Kim, J.-G. Lee, Selfie: Refurbishing unclean samples for robust deep learning, in: International Conference on Machine Learning, 2019.
- [123] L. Huang, C. Zhang, H. Zhang, Self-adaptive training: beyond empirical risk minimization, [ArXiv abs/2002.10319 \(2020\)](#).
- [124] S. Ye, D. Chen, S. Han, J. Liao, Learning with Noisy Labels for Robust Point Cloud Segmentation, in: 2021 IEEE/CVF International Conference on Computer Vision (ICCV), IEEE, Montreal, QC, Canada, 2021, pp. 6423–6432.

- [125] Z. Chen, Z. Li, S. Wang, D. Fu, F. Zhao, Learning from noisy data for semi-supervised 3d object detection, in: Proceedings of the IEEE/CVF International Conference on Computer Vision, 2023, pp. 6929–6939.
- [126] A. Radford, J. W. Kim, C. Hallacy, A. Ramesh, G. Goh, S. Agarwal, G. Sastry, A. Askell, P. Mishkin, J. Clark, G. Krueger, I. Sutskever, Learning transferable visual models from natural language supervision, in: International Conference on Machine Learning, 2021.
- [127] A. Kirillov, E. Mintun, N. Ravi, H. Mao, C. Rolland, L. Gustafson, T. Xiao, S. Whitehead, A. C. Berg, W.-Y. Lo, P. Dollár, R. B. Girshick, Segment anything, 2023 IEEE/CVF International Conference on Computer Vision (ICCV) (2023) 3992–4003.
- [128] R. Chen, Y. Liu, L. Kong, X. Zhu, Y. Ma, Y. Li, Y. Hou, Y. Qiao, W. Wang, Clip2scene: Towards label-efficient 3d scene understanding by clip, 2023 IEEE/CVF Conference on Computer Vision and Pattern Recognition (CVPR) (2023) 7020–7030.
- [129] Z. Chen, B. Li, Bridging the domain gap: Self-supervised 3d scene understanding with foundation models, ArXiv abs/2305.08776 (2023).
- [130] Y.-C. Liu, L. Kong, J. Cen, R. Chen, W. Zhang, L. Pan, K. Chen, Z. Liu, Segment any point cloud sequences by distilling vision foundation models, ArXiv abs/2306.09347 (2023).
- [131] D. Hegde, J. M. J. Valanarasu, V. M. Patel, Clip goes 3d: Leveraging prompt tuning for language grounded 3d recognition, 2023 IEEE/CVF International Conference on Computer Vision Workshops (ICCVW) (2023) 2020–2030.
- [132] S. Peng, K. Genova, ChiyuMaxJiang, A. Tagliasacchi, M. Pollefeys, T. A. Funkhouser, Openscene: 3d scene understanding with open vocabularies, 2023 IEEE/CVF Conference on Computer Vision and Pattern Recognition (CVPR) (2022) 815–824.
- [133] R. Huang, S. Peng, A. Takmaz, F. Tombari, M. Pollefeys, S. Song, G. Huang, F. Engelmann, Segment3d: Learning fine-grained class-agnostic 3d segmentation without manual labels, 2023. arXiv:2312.17232.
- [134] S. Dong, F. Liu, G. Lin, Leveraging large-scale pretrained vision foundation models for label-efficient 3d point cloud segmentation, 2023. arXiv:2311.01989.
- [135] Q. Yu, H. Du, C. Liu, X. Yu, When 3d bounding-box meets sam: Point cloud instance segmentation with weak-and-noisy supervision, 2024 IEEE/CVF Winter Conference on Applications of Computer Vision (WACV) (2023) 3707–3716.
- [136] Y. Zhou, J. Gu, T. Y. Chiang, F. Xiang, H. Su, Point-sam: Promptable 3d segmentation model for point clouds, 2024. arXiv:2406.17741.
- [137] H. Guo, H. Zhu, S. Peng, Y. Wang, Y. Shen, R. Hu, X. Zhou, Sam-guided graph cut for 3d instance segmentation, 2024. arXiv:2312.08372.
- [138] Y. Liu, W. Li, C. Wang, H. Chen, Y. Yuan, When 3d partial points meets sam: Tooth point cloud segmentation with sparse labels, 2024. arXiv:2409.01691.
- [139] Y. Liu, L. Kong, J. Cen, R. Chen, W. Zhang, L. Pan, K. Chen, Z. Liu, Segment any point cloud sequences by distilling vision foundation models, 2023. arXiv:2306.09347.
- [140] A. Osep, T. Meinhardt, F. Ferroni, N. Peri, D. Ramanan, L. Leal-Taixé, Better call sal: Towards learning to segment anything in lidar, 2024. arXiv:2403.13129.
- [141] X. Timoneda, M. Herb, F. Duerr, D. Goehring, F. Yu, Multi-modal nerf self-supervision for lidar semantic segmentation, 2024. arXiv:2411.02969.
- [142] Z. Chen, L. Yang, Y. Li, L. Jing, B. Li, Sam-guided masked token prediction for 3d scene understanding, 2024. arXiv:2410.12158.
- [143] Y. Ganin, V. Lempitsky, Unsupervised domain adaptation by backpropagation, 2015. arXiv:1409.7495.
- [144] R. Moraffah, K. Shu, A. Raglin, H. Liu, Deep causal representation learning for unsupervised domain adaptation, 2019. arXiv:1910.12417.
- [145] R. Li, Q. Jiao, W. Cao, H.-S. Wong, S. Wu, Model adaptation: Unsupervised domain adaptation without source data, 2020 IEEE/CVF Conference on Computer Vision and Pattern Recognition (CVPR) (2020) 9638–9647.
- [146] L. Hu, M. Kan, S. Shan, X. Chen, Duplex generative adversarial network for unsupervised domain adaptation, 2018 IEEE/CVF Conference on Computer Vision and Pattern Recognition (2018) 1498–1507.
- [147] C. He, T. Tan, X. Fan, L. Zheng, Z. Ye, Noise-residual mixup for unsupervised adversarial domain adaptation, Applied Intelligence 53 (2022) 3034–3047.
- [148] C. Qin, H. You, L. Wang, C. C. J. Kuo, Y. Fu, Pointdan: A multi-scale 3d domain adaption network for point cloud representation, 2019. arXiv:1911.02744.
- [149] S. Zhao, Y. Wang, B. Li, B. Wu, Y. Gao, P. Xu, T. Darrell, K. Keutzer, epointda: An end-to-end simulation-to-real domain adaptation framework for lidar point cloud segmentation, Cornell University - arXiv, Cornell University - arXiv (2020).
- [150] L. Yi, B. Gong, T. Funkhouser, Complete & label: A domain adaptation approach to semantic segmentation of lidar point clouds, in: 2021 IEEE/CVF Conference on Computer Vision and Pattern Recognition (CVPR), 2021.
- [151] P. Jiang, S. Saripalli, Lidarnet: A boundary-aware domain adaptation model for point cloud semantic segmentation, in: 2021 IEEE International Conference on Robotics and Automation (ICRA), 2021.
- [152] A. Xiao, J. Huang, D. Guan, F. Zhan, S. Lu, Transfer learning from synthetic to real lidar point cloud for semantic segmentation, Proceedings of the AAAI Conference on Artificial Intelligence (2022) 2795–2803.
- [153] G. Li, G. Kang, X. Wang, Y. Wei, Y. Yang, Adversarially masking synthetic to mimic real: Adaptive noise injection for point cloud segmentation adaptation, in: Proceedings of the IEEE/CVF Conference on Computer Vision and Pattern Recognition (CVPR), 2023, pp. 20464–20474.
- [154] I. Achituve, H. Maron, G. Chechik, Self-supervised learning for domain adaptation on point clouds, 2021 IEEE Winter Conference on Applications of Computer Vision (WACV) (2020) 123–133.
- [155] A. Alliegro, D. Boscaini, T. Tommasi, Joint supervised and self-supervised learning for 3d real world challenges, in: 2020 25th International Conference on Pattern Recognition (ICPR), 2021, pp. 6718–6725.
- [156] J.-B. Grill, F. Strub, F. Altch'e, C. Tallec, P. H. Richemond, E. Buchatskaya, C. Doersch, B. Á. Pires, Z. D. Guo, M. G. Azar, B. Piot, K. Kavukcuoglu, R. Munos, M. Valko, Bootstrap your own latent: A new approach to self-supervised learning, ArXiv abs/2006.07733 (2020).
- [157] A. Cardace, R. Spezialetti, P. Z. Ramirez, S. Salti, L. D. Stefano, Refrec: Pseudo-labels refinement via shape reconstruction for unsupervised 3d domain adaptation, in: 2021 International Conference on 3D Vision (3DV), 2021, pp. 331–341.
- [158] Q. Hu, D. Liu, W. Hu, Density-insensitive unsupervised domain adaptation on 3d object detection, 2023 IEEE/CVF Conference on Computer Vision and Pattern Recognition (CVPR) (2023) 17556–17566.
- [159] X. Peng, X. Zhu, Y. Ma, Cl3d: Unsupervised domain adaptation for cross-lidar 3d detection, in: AAAI Conference on Artificial Intelligence, 2022.
- [160] J. Yang, S. Shi, Z. Wang, H. Li, X. Qi, St3d: Self-training for unsupervised domain adaptation on 3d object detection, 2021 IEEE/CVF Conference on Computer Vision and Pattern Recognition (CVPR) (2021) 10363–10373.
- [161] J. Yang, S. Shi, Z. Wang, H. Li, X. Qi, St3d++: Denoised self-training for unsupervised domain adaptation on 3d object detection, IEEE Transactions on Pattern Analysis and Machine Intelligence 45 (2021) 6354–6371.
- [162] Y. Zeng, C. Wang, Y. Wang, H. Xu, C. Ye, Z. Yang, C. Ma, Learning transferable features for point cloud detection via 3d contrastive co-training, in: Neural Information Processing Systems, 2021.
- [163] Y. You, C. Diaz-Ruiz, Y. Wang, W.-L. Chao, B. Hariharan, M. E. Campbell, K. Q. Weinberger, Exploiting playbacks in unsupervised domain adaptation for 3d object detection in self-driving cars, 2022 International Conference on Robotics and Automation (ICRA) (2021) 5070–5077.
- [164] Y. You, C. P. Phoo, K. Luo, T. Zhang, W.-L. Chao, B. Hariharan, M. E. Campbell, K. Q. Weinberger, Unsupervised adaptation from repeated traversals for autonomous driving, ArXiv abs/2303.15286 (2023).
- [165] C. Saltori, S. Lathuilière, N. Sebe, E. Ricci, F. Galasso, Sf-uda3d: Source-free unsupervised domain adaptation for lidar-based 3d object detection, 2020 International Conference on 3D Vision (3DV) (2020) 771–780.
- [166] L. Shi, Z. Yuan, M. Cheng, Y. Chen, C. Wang, Dfan: Dual-branch feature alignment network for domain adaptation on point clouds, IEEE Transactions on Geoscience and Remote Sensing 60 (2022) 1–12.
- [167] Y. Zhang, C. Zhou, D. Huang, Stal3d: Unsupervised domain adaptation for 3d object detection via collaborating self-training and adversarial

- ial learning, *IEEE Transactions on Intelligent Vehicles* (2024) 1–12.
- [168] Y. Bian, L. Hui, J. Qian, J. Xie, Unsupervised domain adaptation for point cloud semantic segmentation via graph matching, *2022 IEEE/RSJ International Conference on Intelligent Robots and Systems (IROS)* (2022) 9899–9904.
- [169] Y. Wang, N. Zhao, G. H. Lee, Syn-to-real unsupervised domain adaptation for indoor 3d object detection, *arXiv preprint arXiv:2406.11311* (2024).
- [170] X. Peng, R. Chen, F. Qiao, L. Kong, Y.-C. Liu, T. Wang, X. Zhu, Y. Ma, Learning to adapt sam for segmenting cross-domain point clouds, in: *European Conference on Computer Vision*, 2023.
- [171] Y. Wu, M. Xing, Y. Zhang, Y. Xie, Y. Qu, Clip2uda: Making frozen clip reward unsupervised domain adaptation in 3d semantic segmentation, in: *ACM Multimedia*, 2024.
- [172] J. Xu, W. Yang, L. Kong, Y.-C. Liu, R. Zhang, Q. Zhou, B. Fei, Visual foundation models boost cross-modal unsupervised domain adaptation for 3d semantic segmentation, *ArXiv abs/2403.10001* (2024).
- [173] J. Liang, D. Hu, J. Feng, Do we really need to access the source data? source hypothesis transfer for unsupervised domain adaptation, in: *International conference on machine learning*, PMLR, 2020, pp. 6028–6039.
- [174] R. Li, Q. Jiao, W. Cao, H.-S. Wong, S. Wu, Model adaptation: Unsupervised domain adaptation without source data, in: *Proceedings of the IEEE/CVF conference on computer vision and pattern recognition*, 2020, pp. 9641–9650.
- [175] Y. Liu, W. Zhang, J. Wang, Source-free domain adaptation for semantic segmentation, *2021 IEEE/CVF Conference on Computer Vision and Pattern Recognition (CVPR)* (2021) 1215–1224.
- [176] C. Chen, Q. Liu, Y. Jin, Q. Dou, P.-A. Heng, Source-free domain adaptive fundus image segmentation with denoised pseudo-labeling, in: *International Conference on Medical Image Computing and Computer-Assisted Intervention*, 2021.
- [177] M. Litrico, A. D. Bue, P. Morerio, Guiding pseudo-labels with uncertainty estimation for source-free unsupervised domain adaptation, *2023 IEEE/CVF Conference on Computer Vision and Pattern Recognition (CVPR)* (2023) 7640–7650.
- [178] J. Huang, D. Guan, A. Xiao, S. Lu, Model adaptation: Historical contrastive learning for unsupervised domain adaptation without source data, in: *Neural Information Processing Systems*, 2021.
- [179] C. Saltori, E. Krivosheev, S. Lathuilière, N. Sebe, F. Galasso, G. Fiameni, E. Ricci, F. Poiesi, Gippo: Geometrically informed propagation for online adaptation in 3d lidar segmentation, in: *European Conference on Computer Vision*, 2022.
- [180] S. Wang, Y. Tong, X. Shang, Z. Zhang, Multi-confidence guided source-free domain adaption method for point cloud primitive segmentation, *2024 IEEE International Conference on Robotics and Automation (ICRA)* (2024) 737–743.
- [181] J. Duan, Y. Zhang, Y. Qu, Source-free domain adaptation for point cloud semantic segmentation, *2024 IEEE International Conference on Multimedia and Expo (ICME)* (2024) 1–6.
- [182] J. Tian, J. Zhang, W. Li, D. Xu, Vdm-da: Virtual domain modeling for source data-free domain adaptation, *IEEE Transactions on Circuits and Systems for Video Technology* 32 (2021) 3749–3760.
- [183] M. J. Mirza, J. Micorek, H. Possegger, H. Bischof, The norm must go on: Dynamic unsupervised domain adaptation by normalization, *2022 IEEE/CVF Conference on Computer Vision and Pattern Recognition (CVPR)* (2021) 14745–14755.
- [184] H. Lim, B. Kim, J. Choo, S. Choi, Ttn: A domain-shift aware batch normalization in test-time adaptation, *ArXiv abs/2302.05155* (2023).
- [185] S. Niu, J. Wu, Y. Zhang, Y. Chen, S. D. Zheng, P. Zhao, M. Tan, Efficient test-time model adaptation without forgetting, in: *International Conference on Machine Learning*, 2022.
- [186] D. Wang, E. Shelhamer, S. Liu, B. A. Olshausen, T. Darrell, Tent: Fully test-time adaptation by entropy minimization, in: *International Conference on Learning Representations*, 2021.
- [187] M. Döbler, R. A. Marsden, B. Yang, Robust mean teacher for continual and gradual test-time adaptation, *2023 IEEE/CVF Conference on Computer Vision and Pattern Recognition (CVPR)* (2022) 7704–7714.
- [188] D. Chen, D. Wang, T. Darrell, S. Ebrahimi, Contrastive test-time adaptation, *2022 IEEE/CVF Conference on Computer Vision and Pattern Recognition (CVPR)* (2022) 295–305.
- [189] S. Goyal, M. Sun, A. Raghunathan, Z. Kolter, Test-time adaptation via conjugate pseudo-labels, *ArXiv abs/2207.09640* (2022).
- [190] I. Shin, Y.-H. Tsai, B. Zhuang, S. Schuster, B. Liu, S. Garg, I. S. Kweon, K.-J. Yoon, Mm-tta: multi-modal test-time adaptation for 3d semantic segmentation, in: *Proceedings of the IEEE/CVF Conference on Computer Vision and Pattern Recognition*, 2022, pp. 16928–16937.
- [191] H. Cao, Y. Xu, J. Yang, P. Yin, S. Yuan, L. Xie, Multi-modal continual test-time adaptation for 3d semantic segmentation, *2023 IEEE/CVF International Conference on Computer Vision (ICCV)* (2023) 18763–18773.
- [192] T. Zou, S. Qu, Z. Li, A. Knoll, L. He, G. Chen, C. Jiang, Hgl: Hierarchical geometry learning for test-time adaptation in 3d point cloud segmentation, in: *European Conference on Computer Vision*, Springer, 2025, pp. 19–36.
- [193] H. Shim, C. Kim, E. Yang, Cloudfixer: Test-time adaptation for 3d point clouds via diffusion-guided geometric transformation, in: *European Conference on Computer Vision*, 2024.
- [194] J. Jiang, Q. Zhou, Y. Li, X. Zhao, M. Wang, L. Ma, J. Chang, J. J. Zhang, X. Lu, Pcotta: Continual test-time adaptation for multi-task point cloud understanding, 2024.
- [195] A. S. Hatem, Y. Qian, Y. Wang, Point-tta: Test-time adaptation for point cloud registration using multitask meta-auxiliary learning, *2023 IEEE/CVF International Conference on Computer Vision (ICCV)* (2023) 16448–16458.
- [196] A. S. Hatem, Y. Qian, Y. Wang, Test-time adaptation for point cloud up-sampling using meta-learning, *2023 IEEE/RSJ International Conference on Intelligent Robots and Systems (IROS)* (2023) 1284–1291.
- [197] X. Liu, Y. Su, T. Hu, Q. Yang, B. Liu, Y. Deng, H. Tang, Z. Tang, J. Fang, Q. Guo, Neural network guided interpolation for mapping canopy height of china’s forests by integrating gedi and icesat-2 data, *Remote Sensing of Environment* 269 (2022) 112844.
- [198] I. Fayad, D. Ienco, N. Baghdadi, R. Gaetano, C. A. Alvares, J. L. Stape, H. Ferrazo Scolforo, G. Le Maire, A cnn-based approach for the estimation of canopy heights and wood volume from gedi waveforms, *Remote Sensing of Environment* 265 (2021) 112652.
- [199] X. Zhu, S. Nie, C. Wang, X. Xi, D. Li, G. Li, P. Wang, D. Cao, X. Yang, Estimating terrain slope from icesat-2 data in forest environments, *Remote Sensing* 12 (2020).
- [200] X. Zhu, S. Nie, C. Wang, X. Xi, J. Lao, D. Li, Consistency analysis of forest height retrievals between gedi and icesat-2, *Remote Sensing of Environment* 281 (2022) 113244.
- [201] M. Pourshamsi, J. Xia, N. Yokoya, M. Garcia, M. Lavalley, E. Pottier, H. Balzter, Tropical forest canopy height estimation from combined polarimetric sar and lidar using machine-learning, *ISPRS Journal of Photogrammetry and Remote Sensing* 172 (2021) 79–94.
- [202] X. Lin, M. Xu, C. Cao, Y. Dang, B. Bashir, B. Xie, Z. Huang, Estimates of forest canopy height using a combination of icesat-2/atlas data and stereo-photogrammetry, *Remote Sensing* 12 (2020).
- [203] I. Dorado-Roda, A. Pascual, S. Godinho, C. A. Silva, B. Botequim, P. Rodríguez-González, E. González-Ferreiro, J. Guerra-Hernández, Assessing the accuracy of gedi data for canopy height and aboveground biomass estimates in mediterranean forests, *Remote Sensing* 13 (2021).
- [204] P. Potapov, X. Li, A. Hernandez-Serna, A. Tyukavina, M. C. Hansen, A. Kommareddy, A. Pickens, S. Turubanova, H. Tang, C. E. Silva, J. Armston, R. Dubayah, J. B. Blair, M. Hofton, Mapping global forest canopy height through integration of gedi and landsat data, *Remote Sensing of Environment* 253 (2021) 112165.
- [205] Z. Xi, H. Xu, Y. Xing, W. Gong, G. Chen, S. Yang, Forest canopy height mapping by synergizing icesat-2, sentinel-1, sentinel-2 and topographic information based on machine learning methods, *Remote Sensing* 14 (2022).
- [206] C. Sothe, A. Gonsamo, R. B. Lourenço, W. A. Kurz, J. Snider, Spatially continuous mapping of forest canopy height in canada by combining gedi and icesat-2 with palsar and sentinel, *Remote Sensing* 14 (2022).
- [207] C. Wang, A. J. Elmore, I. Numata, M. A. Cochrane, S. Lei, C. R. Hakkenberg, Y. Li, Y. Zhao, Y. Tian, A framework for improving wall-to-wall canopy height mapping by integrating gedi lidar, *Remote Sensing* 14 (2022).
- [208] N. Lang, N. Kalischek, J. Armston, K. Schindler, R. Dubayah, J. D. Wegner, Global canopy height regression and uncertainty estimation from gedi lidar waveforms with deep ensembles, *Remote Sensing of*

- Environment 268 (2022) 112760.
- [209] D. Carcereri, P. Rizzoli, L. Dell'Amore, J.-L. Bueso-Bello, D. Ienco, L. Bruzzone, Generation of country-scale canopy height maps over gabon using deep learning and tandem-x insar data, *Remote Sensing of Environment* 311 (2024) 114270.
- [210] M. Weber, C. Beneke, C. Wheeler, Unified deep learning model for global prediction of aboveground biomass, canopy height and cover from high-resolution, multi-sensor satellite imagery, 2024. [arXiv:2408.11234](https://arxiv.org/abs/2408.11234).
- [211] G. Fan, F. Yan, X. Zeng, Q. Xu, R. Wang, B. Zhang, J. Zhou, L. Nan, J. Wang, Z. Zhang, J. Wang, First mapping the canopy height of primeval forests in the tallest tree area of asia, 2024. [arXiv:2404.14661](https://arxiv.org/abs/2404.14661).
- [212] I. Fayad, P. Ciaï, M. Schwartz, J.-P. Wigneron, N. Baghdadi, A. de Truchis, A. d'Aspremont, F. Frappart, S. Saatchi, E. Sean, A. Pellissier-Tanon, H. Bazzi, Hy-tec: a hybrid vision transformer model for high-resolution and large-scale mapping of canopy height, *Remote Sensing of Environment* 302 (2024) 113945.
- [213] J. Lao, C. Wang, X. Zhu, X. Xi, S. Nie, J. Wang, F. Cheng, G. Zhou, Retrieving building height in urban areas using icesat-2 photon-counting lidar data, *International Journal of Applied Earth Observation and Geoinformation* 104 (2021) 102596.
- [214] Y. Cao, Q. Weng, A deep learning-based super-resolution method for building height estimation at 2.5 m spatial resolution in the northern hemisphere, *Remote Sensing of Environment* 310 (2024) 114241.
- [215] X. Li, Y. Zhou, P. Gong, K. C. Seto, N. Clinton, Developing a method to estimate building height from sentinel-1 data, *Remote Sensing of Environment* 240 (2020) 111705.
- [216] X. Ma, G. Zheng, C. Xu, L. M. Moskal, P. Gong, Q. Guo, H. Huang, X. Li, Y. Pang, C. Wang, H. Xie, B. Yu, B. Zhao, Y. Zhou, A global product of fine-scale urban building height based on spaceborne lidar, 2023. [arXiv:2310.14355](https://arxiv.org/abs/2310.14355).
- [217] X. Ma, G. Zheng, X. Chi, L. Yang, Q. Geng, J. Li, Y. Qiao, Mapping fine-scale building heights in urban agglomeration with spaceborne lidar, *Remote Sensing of Environment* 285 (2023) 113392.
- [218] H. G. Kamath, M. Singh, L. A. Magruder, Z.-L. Yang, D. Niyogi, Globus: Global building heights for urban studies, [ArXiv abs/2205.12224](https://arxiv.org/abs/2205.12224) (2022).
- [219] D. Frantz, F. Schug, A. Okujeni, C. Navacchi, W. Wagner, S. van der Linden, P. Hostert, National-scale mapping of building height using sentinel-1 and sentinel-2 time series, *Remote Sensing of Environment* 252 (2021) 112128.
- [220] G. Sialelli, T. Peters, J. D. Wegner, K. Schindler, Agbd: A global-scale biomass dataset, 2024. [arXiv:2406.04928](https://arxiv.org/abs/2406.04928).
- [221] M. J. Campbell, P. E. Dennison, K. L. Kerr, S. C. Brewer, W. R. Anderegg, Scaled biomass estimation in woodland ecosystems: Testing the individual and combined capacities of satellite multispectral and lidar data, *Remote Sensing of Environment* 262 (2021) 112511.
- [222] L. Gao, G. Chai, X. Zhang, Above-ground biomass estimation of plantation with different tree species using airborne lidar and hyperspectral data, *Remote Sensing* 14 (2022).
- [223] F. Jiang, H. Sun, K. Ma, L. Fu, J. Tang, Improving aboveground biomass estimation of natural forests on the tibetan plateau using spaceborne lidar and machine learning algorithms, *Ecological Indicators* 143 (2022) 109365.
- [224] M. Vázquez-Alonso, D. L. Lentz, N. P. Dunning, C. Carr, A. Anaya Hernández, K. Reese-Taylor, Lidar-based aboveground biomass estimations for the maya archaeological site of yaxnohcah, campeche, mexico, *Remote Sensing* 14 (2022).
- [225] L. Duncanson, J. R. Kellner, J. Armston, R. Dubayah, D. M. Minor, S. Hancock, S. P. Healey, P. L. Patterson, S. Saarela, S. Marselis, C. E. Silva, J. Bruening, S. J. Goetz, H. Tang, M. Hofton, B. Blair, S. Luthcke, L. Fatoyinbo, K. Abernethy, A. Alonso, H.-E. Andersen, P. Aplin, T. R. Baker, N. Barbier, J. F. Bastin, P. Biber, P. Boeckx, J. Boagaert, L. Boschetti, P. B. Boucher, D. S. Boyd, D. F. Burslem, S. Calvo-Rodriguez, J. Chave, R. L. Chazdon, D. B. Clark, D. A. Clark, W. B. Cohen, D. A. Coomes, P. Corona, K. Cushman, M. E. Cutler, J. W. Dalling, M. Dalponte, J. Dash, S. de Miguel, S. Deng, P. W. Ellis, B. Erasmus, P. A. Fekety, A. Fernandez-Landa, A. Ferraz, R. Fischer, A. G. Fisher, A. García-Abril, T. Gobakken, J. M. Hacker, M. Heurich, R. A. Hill, C. Hopkins, H. Huang, S. P. Hubbell, A. T. Hudak, A. Huth, B. Imbach, K. J. Jeffery, M. Katoh, E. Kearsley, D. Kenfack, N. Kljun, N. Knapp, K. Král, M. Krůček, N. Labrière, S. L. Lewis, M. Longo, R. M. Lucas, R. Main, J. A. Manzanera, R. V. Martínez, R. Mathieu, H. Memiaghe, V. Meyer, A. M. Mendoza, A. Moneris, P. Montesano, F. Morsdorf, E. Næsset, L. Naidoo, R. Nilus, M. O'Brien, D. A. Orwig, K. Papathanassiou, G. Parker, C. Philipson, O. L. Phillips, J. Pisek, J. R. Poulsen, H. Pretzsch, C. Rüdiger, S. Saatchi, A. Sanchez-Azofeifa, N. Sanchez-Lopez, R. Scholes, C. A. Silva, M. Simard, A. Skidmore, K. Stereńczak, M. Tanase, C. Torresan, R. Valbuena, H. Verbeeck, T. Vrska, K. Wessels, J. C. White, L. J. White, E. Zahabu, C. Zraggen, Aboveground biomass density models for nasa's global ecosystem dynamics investigation (gedi) lidar mission, *Remote Sensing of Environment* 270 (2022) 112845.
- [226] Y. Deng, J. Pan, J. Wang, Q. Liu, J. Zhang, Mapping of forest biomass in shangri-la city based on lidar technology and other remote sensing data, *Remote Sensing* 14 (2022).
- [227] S. Qin, S. Nie, Y. Guan, D. Zhang, C. Wang, X. Zhang, Forest emissions reduction assessment using airborne lidar for biomass estimation, *Resources, Conservation and Recycling* 181 (2022) 106224.
- [228] J. Guerra-Hernández, L. L. Narine, A. Pascual, E. Gonzalez-Ferreiro, B. Bottequin, L. Malambo, A. Neuenschwander, S. C. Popescu, S. Godinho, Aboveground biomass mapping by integrating icesat-2, sentinel-1, sentinel-2, alos2/palsar2, and topographic information in mediterranean forests, *GIScience & Remote Sensing* 59 (2022) 1509–1533.
- [229] S. Oehmcke, L. Li, K. Trepekli, J. C. Revenga, T. Nord-Larsen, F. Gieseke, C. Igel, Deep point cloud regression for above-ground forest biomass estimation from airborne lidar, *Remote Sensing of Environment* 302 (2024) 113968.
- [230] Y. Shendryk, Fusing gedi with earth observation data for large area aboveground biomass mapping, *International Journal of Applied Earth Observation and Geoinformation* 115 (2022) 103108.
- [231] M. Muszynski, L. Klein, A. F. da Silva, A. P. Atluri, C. Gomes, D. Szwarcman, G. Singh, K. Gu, M. Zortea, N. Simumba, P. Fraccaro, S. Singh, S. Meliksetian, C. Watson, D. Kimura, H. Srinivasan, Fine-tuning of geospatial foundation models for aboveground biomass estimation, 2024. [arXiv:2406.19888](https://arxiv.org/abs/2406.19888).
- [232] X. Zou, J. Yang, H. Zhang, F. Li, L. Li, J. Wang, L. Wang, J. Gao, Y. J. Lee, Segment everything everywhere all at once, in: A. Oh, T. Naumann, A. Globerson, K. Saenko, M. Hardt, S. Levine (Eds.), *Advances in Neural Information Processing Systems*, volume 36, Curran Associates, Inc., 2023, pp. 19769–19782.
- [233] O. Russakovsky, J. Deng, H. Su, J. Krause, S. Satheesh, S. Ma, Z. Huang, A. Karpathy, A. Khosla, M. S. Bernstein, A. C. Berg, L. Fei-Fei, Imagenet large scale visual recognition challenge, *International Journal of Computer Vision* 115 (2014) 211–252.
- [234] S. Liu, K. Liu, W. Zhu, Y. Shen, C. Fernandez-Granda, Adaptive early-learning correction for segmentation from noisy annotations, in: 2022 IEEE/CVF Conference on Computer Vision and Pattern Recognition (CVPR), 2022, pp. 2596–2606.
- [235] J. E. Vargas-Munoz, S. Srivastava, D. Tuia, A. X. Falcão, Openstreetmap: Challenges and opportunities in machine learning and remote sensing, *IEEE Geoscience and Remote Sensing Magazine* 9 (2021) 184–199.
- [236] K. Li, R. Liu, X. Cao, X. Bai, F. Zhou, D. Meng, Z. Wang, Segearth-ov: Towards training-free open-vocabulary segmentation for remote sensing images, 2024. [arXiv:2410.01768](https://arxiv.org/abs/2410.01768).
- [237] Z. Li, W. Han, Y. Zhang, Q. Fu, J. Li, L. Qin, R. Dong, H. Sun, Y. Deng, L. Yang, Learning spatiotemporal dynamics with a pretrained generative model, *Nature Machine Intelligence* (2024).
- [238] M. J. Allen, F. Dorr, J. A. G. Mejia, L. Martínez-Ferrer, A. Jungbluth, F. Kalaitzis, R. Ramos-Pollán, M3leo: A multi-modal, multi-label earth observation dataset integrating interferometric sar and multispectral data, in: *The Thirty-eight Conference on Neural Information Processing Systems Datasets and Benchmarks Track*, 2024.
- [239] X. Xue, G. Wei, H. Chen, H. Zhang, F. Lin, C. Shen, X. X. Zhu, Reo-vm: Transforming vlm to meet regression challenges in earth observation, 2024. [arXiv:2412.16583](https://arxiv.org/abs/2412.16583).